# Accepted Manuscript


Structure-activity relationships of 2, 4-disubstituted pyrimidines as dual ERα/ VEGFR-2 ligands with anti-breast cancer activity

Guoshun Luo, Zhichao Tang, Kejing Lao, Xinyu Li, Qidong You, Hua Xiang

PII: S0223-5234(18)30253-8

DOI: 10.1016/j.ejmech.2018.03.018

Reference: EJMECH 10283

To appear in: *European Journal of Medicinal Chemistry*

Received Date: 28 December 2017

Revised Date: 26 February 2018

Accepted Date: 5 March 2018

Please cite this article as: G. Luo, Z. Tang, K. Lao, X. Li, Q. You, H. Xiang, Structure-activity relationships of 2, 4-disubstituted pyrimidines as dual ERα/VEGFR-2 ligands with anti-breast cancer activity, *European Journal of Medicinal Chemistry* (2018), doi: 10.1016/j.ejmech.2018.03.018.

# Graphical abstract

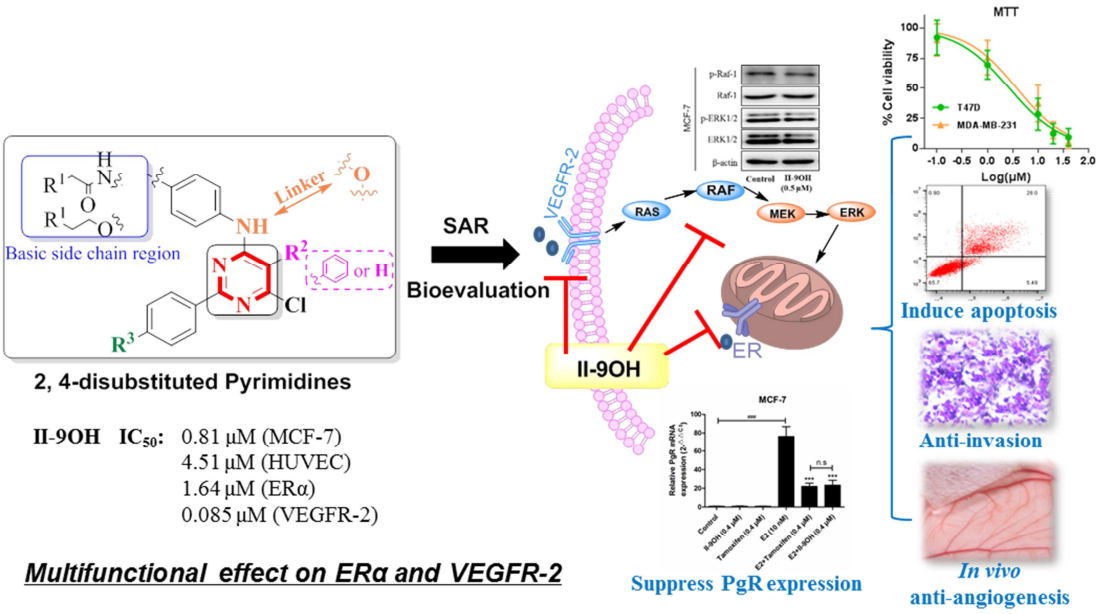


**II-9OH** $IC_{50}$: 0.81 μM (MCF-7)
4.51 μM (HUVEC)
1.64 μM (ERα)
0.085 μM (VEGFR-2)

***Multifunctional effect on ERα and VEGFR-2***

# Structure-Activity Relationships of 2, 4-disubstituted Pyrimidines as Dual ERα/VEGFR-2 Ligands with Anti-Breast Cancer Activity

Guoshun Luo[a,b], Zhichao Tang[a,b], Kejing Lao[c], Xinyu Li[a,b], Qidong You[a,b], Hua Xiang[a,b]*

[a]*State Key Laboratory of Natural Medicines, Jiangsu Key Laboratory of Drug Design and Optimization, China Pharmaceutical University, Nanjing 210009,China*

[b]*Department of Medicinal Chemistry, School of Pharmacy, China Pharmaceutical University, Nanjing 210009, China*

[c]*Institute of Basic and Translational Medicine, and School of Basic Medical Science, Xi'an Medical University, No.1 Xinwang Road, Xi'an, 710021, China*

* Corresponding author. Tel.: +86 025 83271096; Fax: +86 025 83271096 (H. Xiang).

E-mail addresses: xianghua@cpu.edu.cn (H. Xiang)

**Abstract**

Both ERα and VEGFR-2 are important targets for cancer therapies. Here a series of 2, 4-disubstituted pyrimidine derivatives were designed, synthesized and evaluated as dual ERα/VEGFR-2 ligands. Most of the derivatives exhibited potent activities in both enzymatic and cellular assays. Structure-activity relationship studies showed that a hydrogen-bonding interaction in the head section is important factors for the enhancement of ERα-binding affinity. The most potent compound **II-9OH**, an analog of 2-(4-hydroxylphenyl)pyrimidine, was 19-fold more efficacious than tamoxifen in MCF-7 cancer cells and exhibited the best ERα binding affinity ($IC_{50}$=1.64 μM) as well as excellent VEGFR-2 inhibition ($IC_{50}$=0.085 μM). Furthermore, this dual targeted compound **II-9OH** exerted significantly antiestrogenic property via suppressing the expression of progesterone receptor (PgR) mRNA in MCF-7 cells and also showed obvious *in vivo* angiogenesis inhibitory effects in CAM assay. An induction of apoptosis and a decrease in cell migration, accompanied by transduction inhibition of Raf-1/MAPK/ERK pathway, were observed in MCF-7 cells after treatment with **II-9OH**, suggesting that **II-9OH** is a promising candidate for the development of multifunctional agents targeting ERα and VEGFR-2 in the therapy of some breast cancers.

**Keywords:** 2, 4-disubstituted Pyrimidines; ERα; VEGFR-2; antiangiogenesis; anti-breast cancer.

## 1. Introduction

Breast cancer (BC) is one of the most common types of cancer and the most frequent cause of cancer death among females worldwide. Estrogen receptor alpha (ERα) positive breast cancer accounts for approximately 70% of these cases [1]. Selective estrogen receptor modulators (SERMs) which act as antagonists in breast tissue but agonists in other tissues such as cardiovascular system and bone represent first-line treatment for ER+ patients [2, 3]. Tamoxifen, the first generation of SERM, is the most commonly used drug for the treatment of estrogen receptor positive breast cancer and has been in clinical use for four decades [4, 5]. Since then, multiple additional SERMs with various scaffolds mimicking Tamoxifen have been developed for the treatment or prevention of breast cancer [5-8]. Many alternative scaffolds for ER modulators have also been reported, e.g., the heterocyclic propylpyrazoletriol (PPT) and *m*-carborane-containing compound (Fig. 1A) [9-11].

However, up to 50% of patients either do not respond or acquire resistance within 5

years of SERM treatment [12]. Multiple mechanisms contribute to the development of an ER+ and treatment resistant (TR) phenotype, in which growth is endocrine independent, including alterations in crosstalk between ER and growth factor-mediated signaling pathways [13, 14] Increasing studies have revealed that aberrant activation of Raf-1/MAPK/ERK pathway interplays with ER in regulating estrogen-dependent gene expression and is widely observed in the endocrine resistance [15, 16]. Vascular endothelial growth factor receptor-2 (VEGFR-2) is a member of the receptor tyrosine kinase (RTK) family and the upstream effector of Raf-1/MAPK/ERK signaling in promoting cell proliferation, migration and angiogenesis in cancer [17]. Recently, the combination of Tamoxifen with Brivanib, a VEGFR-2 inhibitor, was reported not only to maximize therapeutic efficacy but also to retard SERM resistant tumor growth [18]. Therefore, development of a multiple ligand of ER and VEGFR-2, exerting enhanced activity against BC with fewer disadvantages is highly needed.

In the course of identifying various chemical fragments that could serve as a scaffold for new antitumor agents, the literature revealed that pyrimidine is an essential druglike nucleus bearing enormous biological applicability and has the ability to interact with diverse target sites i.e., enzymes, receptors, DNA, protein targets, etc [19, 20]. Particularly, the pyrimidine ring was widely used as a common skeleton in various kinases including VEGFR-2 and proved to exhibit potent anticancer activities (Fig. 1B) [21-24]. As our ongoing interest to explore different scaffold structures as multiple ligands of ER and VEGFR-2 [25, 26], we designed and synthesized a series of 2, 4-disubstituted pyrimidine derivatives with basic side chain to inhibit the proliferation of breast cancer cells (Fig. 1C). Firstly, the pyrimidine moiety was utilized as a core scaffold to initiate the interactions with ERα ligand-binding domain (LBD) as *m*-carborane and pyrazole did as well as the interactions with VEGFR-2 kinase hinge as adenine did [11, 22]. Then a substituted aromatic ring was introduced to the 2- or 5-position to occupy the hydrophobic pocket of ER receptor and VEGFR-2 kinase. Next, various N, N-dialkylamino containing side chains were introduced at *para*-position of 4-phenyl substituent, which is the most noteworthy feature of SERMs and serves to inhibit the binding of co-activators by moving helix-12 of the receptor to an unfavorable position [27]. Finally, our exploration focused on the biological effect of the bridging atoms between the phenyl and pyrimidine moieties, in addition to the established NH linker, bioisosteric group O atom was also employed. Herein, we disclosed the synthesis of 24 novel pyrimidine-based analogs and preliminary pharmacological data from receptor binding, enzyme inhibition as well as antiproliferation assays. A lead compound was identified and its antiangiogenic activity, anti-estrogenic property together with the effect on VEGFR-2/Raf-1/MAPK/ERK

signaling pathway were further evaluated. Molecule docking was also carried out for ERα and VEGFR-2 in order to explore the potential binding mode of the novel dual-action inhibitor.

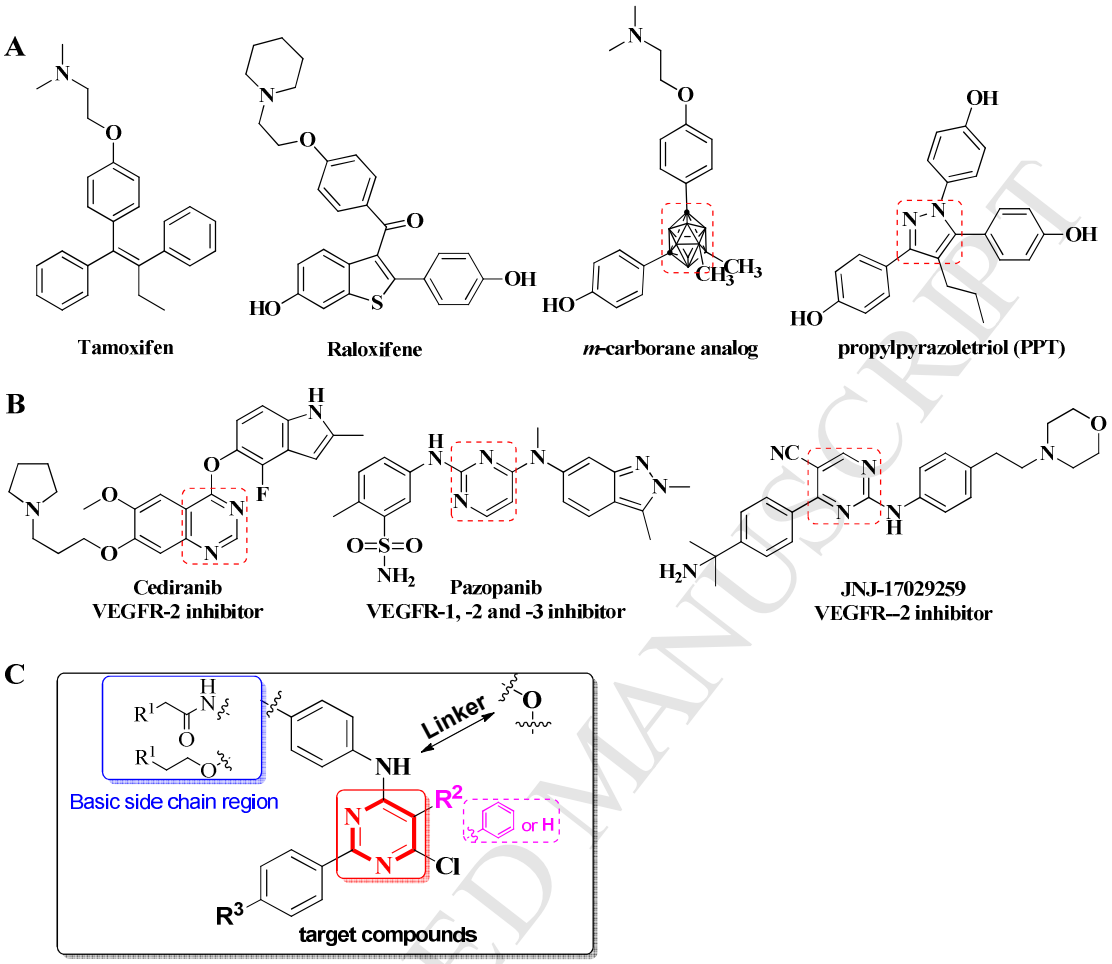


**Fig. 1.** Structures of selective estrogen receptor modulators (A), pyrimidine-based VEGFR-2 inhibitors (B) and proposed pyrimidine-based ERα/VEGFR-2 Ligands (C).

## 2. Results and discussion

### 2.1 Chemistry

The synthesis of compounds **I-1**~**I-9** and **II-1**~**II-9** is described in Schemes 1. The key intermediates **6a-6b** were prepared from commercially available 4-methoxybenzaldehyde according to literature procedure in high yields [28]. Briefly, 4-methoxybenzaldehyde reacted with hydroxylamine under reflux to yield benzonitrile **2**, which was then converted to the corresponding 4-methoxybenzimidamide **3**. Further treatment of **3** with diethyl malonates **4a** or **5a** in reflux MeOH gave cyclized compound **5a** or **5b**, respectively. Next, 4, 6-dihydroxypyrimidine **5a** and **5b** were then subjected to a selective chlorination in the presence of $POCl_3$ to provide the key intermediates **6a** and **6b**. Finally, combination of different side chains with compound **6a** and **6b** afforded the target compounds **I-1**~**I-9** and

**II-1**~**II-9**, respectively. Compounds **II-4OH**, **II-5OH** and **II-9OH** were prepared from their corresponding methoxy compounds **II-4**, **II-5** and **II-9** by demethylation with $BBr_3$ (Scheme 2).

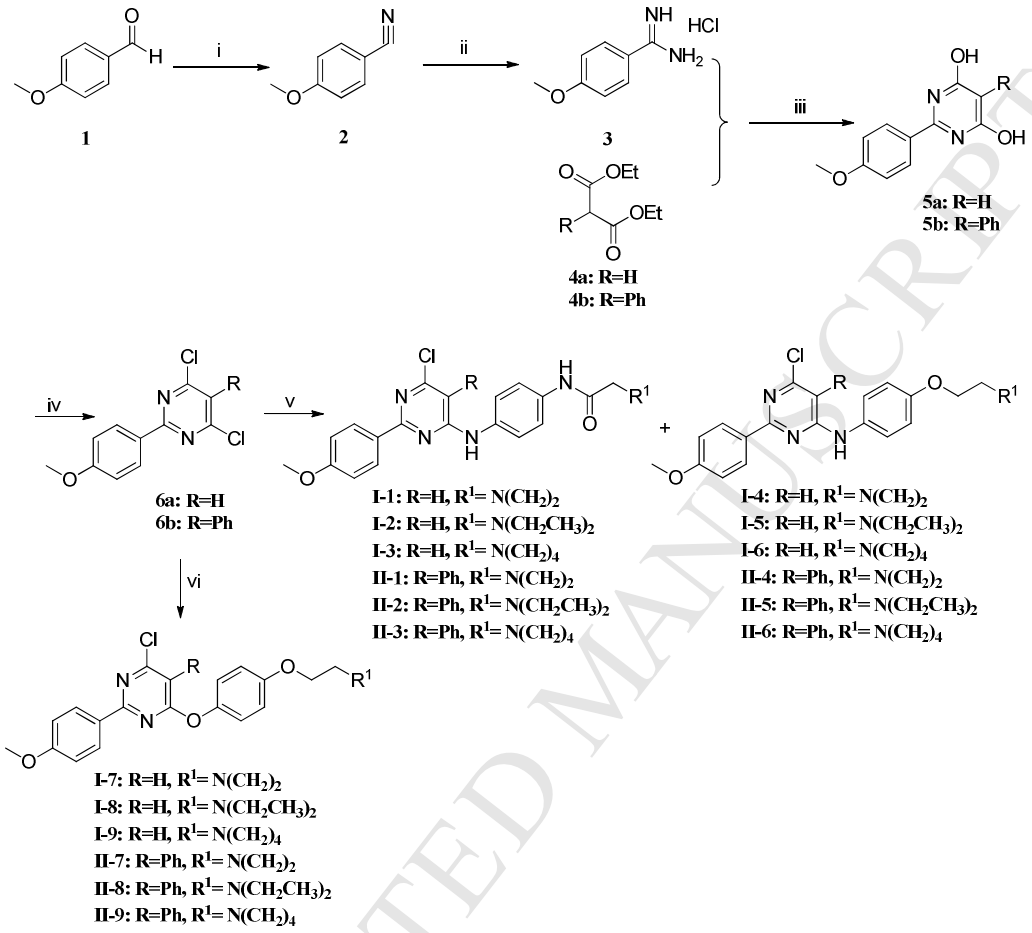


**Scheme 1.** Synthetic routes of **I-1**~**I-9** and **II-1**~**II-9**. Reagents and conditions: (i) $NH_2OH{\cdot}HCl$, DMSO, 100 °C, 0.5 h; (ii) dry methanol, $CH_3ONa$, rt, 48 h; $NH_4Cl$, rt, 24 h; (iii) dry methanol, $CH_3ONa$, reflux, 4 h; (iv) $POCl_3$, 110 °C, 5 h; (v) dry dioxane, $Pd(PPh_3)_2Cl_2$, $K_2CO_3$, 100 °C, 8 h; (vi) dry DMF, $K_2CO_3$, 80 °C, 4 h.

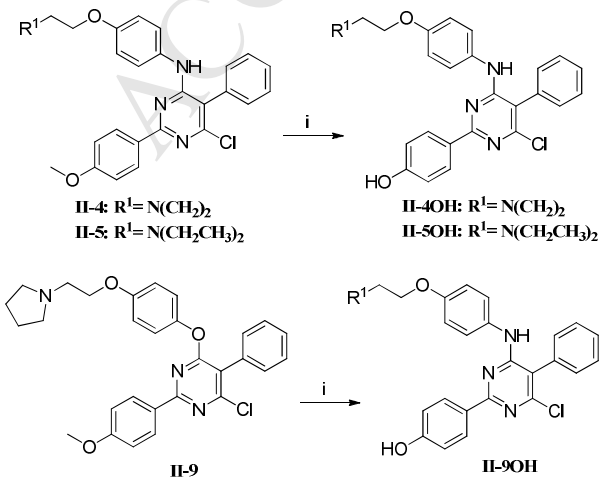

**Scheme 2.** Synthetic routes of **II-4OH**, **II-5OH** and **II-9OH**. Reagents and conditions: (i) dry dichloromethane, $BBr_3$, 0 °C-rt, 4 h.

2.2. Biological evaluation.

2.2.1. ERα binding affinity assay and antiproliferative activity.

The ERα binding affinities of title molecules were initially evaluated using ER-α competitor assay kit (Polar Screen ER-α Competitor Assay Kit, Green, Life Technology). Additionally, in order to verify the probability of synthesized compounds as novel ERα antagonists, the potential cytotoxic effects were also investigated in MCF-7 cell (ER+) using MTT assay. It is known that long term treatment of tamoxifen will stimulate endometrial cell growth and induce endometrial cancer; antiproliferative activity of new compounds on endometrial cells was also measured. For comparison, clinically approved SERMs tamoxifen and raloxifene was used as the positive control in these two assays.

These result data can be analyzed in two groups, 5-hydrogen analogues (**I-1**~**I-9**) and 5-phenyl substituted analogues (**II-1**~**II-9**), and are depicted in Table 1. As a global observation, most of the 2, 4-disubstituted pyrimidines showed promising binding affinities with more than 50% inhibition at 10 μM indicating that pyrimidine scaffold could favorably bind to ERα ligand-binding domain. Most 5-hydrogen prototypes were more active in ERα binding assay than their phenyl-substituted counterpart compounds except **II-9** which exhibited the best ERα binding affinity ($IC_{50}$= 4.57 μM). Compounds **I-4**, **II-4**, **II-5**, and **II-6** showed significant in vitro cytotoxicity against both MCF-7 and Ishikawa cells that surpassed those of clinical SERM tamoxifen and raloxifene. It was interesting to find that compounds (**I-4**, **II-4**, **II-5** and **II-6**) which were less potent in ERα binding assay manifested promising anti-proliferative activity against MCF-7 cells with $IC_{50}$ values of 3.54, 7.56, 8.59 and 7.84 μM respectively, which confirmed that the obtained antiproliferative activity was not only through ERα but a multi-target effect. Investigation on the side chain revealed an unfavorite in acetamide side chain in MCF-7 compared with the ethoxy chain and a decrease in activity was observed (**I-1** vs **I-4**, **I-2** vs **I-5**, **II-1** vs **II-4**, **II-2** vs **II-5** and **II-3** vs **II-6**). And similar trend was also seen in Ishikawa cells (**I-1** vs **I-4**, **I-2** vs **I-5**, **I-3** vs **I-6**, **II-1** vs **II-4**, **II-2** vs **II-5** and **II-3** vs **II-6**).

**Table 1**

ERα binding affinity and antiproliferation activity of compounds **-1~I-9**, **II-1~II-9**, **II-4OH**, **II-5OH** and **II-9OH**

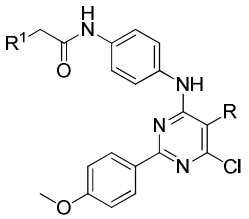

**I-1~I-3**
**II-1~II-3**

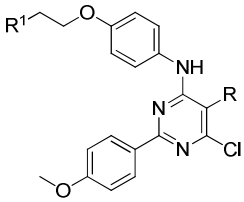

**I-4~I-6**
**II-4~II-6**

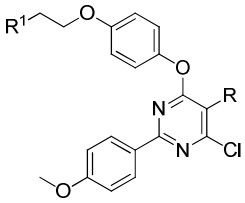

**I-7~I-9**
**II-7~II-9**

| Cmpd | R | $R^1$ | ERα binding affinity[a] | | Antiproliferation ($IC_{50}$, μM)[c] | |
|---|---|---|---|---|---|---|
| | | | Inh% at 10 μM | $IC_{50}$ (μM) | MCF-7 | Ishikawa |
| **I-1** | H |  | 64.32 | ND[b] | >40 | >40 |
| **I-2** | H |  | 66.64 | ND | >40 | 5.81 |
| **I-3** | H |  | 80.47 | 2.86 | 23.35 | 18.35 |
| **I-4** | H |  | 65.35 | ND | 3.54 | 5.67 |
| **I-5** | H |  | 77.22 | 4.74 | 36.82 | 11.67 |
| **I-6** | H |  | 65.97 | ND | 43.7 | 17.28 |
| **I-7** | H |  | 74.53 | 5.96 | >40 | >40 |
| **I-8** | H |  | 77.69 | 5.13 | 49.61 | 24.86 |
| **I-9** | H |  | 72.74 | 6.22 | 21.32 | 25.51 |
| **II-1** | Ph |  | 55.39 | ND | 17.66 | 17.14 |
| **II-2** | Ph |  | 65.76 | ND | >40 | >40 |
| **II-3** | Ph |  | 60.59 | ND | >40 | >40 |
| **II-4** | Ph |  | 69.47 | ND | 7.56 | 6.34 |
| **II-5** | Ph |  | 42.33 | ND | 8.59 | 9.98 |
| **II-6** | Ph |  | 51.68 | ND | 7.84 | 3.81 |

| | | | | | | |
|---|---|---|---|---|---|---|
| **II-7** | Ph |  | 58.17 | ND | 21.75 | 17.72 |
| **II-8** | Ph |  | 58.79 | ND | >40 | 23.46 |
| **II-9** | Ph |  | 84.87 | 2.17 | 32.43 | 14.12 |
| **II-4OH** | | 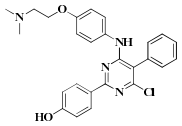 | 80.44 | 3.42 | 33.1 | 37.13 |
| **II-5OH** | | 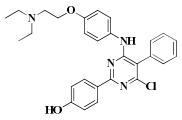 | 54.23 | ND | 35.6 | 12.02 |
| **II-9OH** | | 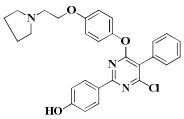 | 90.15 | 1.64 | 0.81 | 5.93 |
| **Tamoxifen** | - | - | 92.36 | 1.42 | 15.46 | 26.52 |
| **Raloxifene** | - | - | - | - | 13.18 | 24.37 |

[a]Percent inhibition of each compound was calculated from the polarization values. The $IC_{50}$ values are calculated when the Inh% at 10 μM is >70%.

[b]ND stands for not determined

[c]$IC_{50}$: concentration that inhibits 50% of cell growth

It is known that the hydrogen bonds formed between the two hydroxyl group of estradiol (endogenous ERα ligand) and Glu353, Arg394 and His524 are important and required to keep the conformation stable when estradiol binds to ERα [29]. The ability to form hydrogen bonds with these three key amino acids is widely accepted as required to identify ERα ligands. For the purpose of exploring the SAR of substituent group in 2-phenyl ring, we next studied the hydrogen donor group on activity by designing compounds **II-4OH**, **II-5OH** and **II-9OH** (Table 1). It was supposed that hydroxyl group at C-4' position of 2-phenyl substituent would form more hydrogen bonds with essential amino acids than methoxyl group in the ligand binding domain of ERα. Expectedly, it is obvious to note that hydroxyl containing derivatives **II-4OH** ($IC_{50}$=3.42 μM) and **II-9OH** ($IC_{50}$=1.64 μM) possessed apparently better affinities to ERα than methoxyl substituted lead compound **II-4** and **II-9** ($IC_{50}$=2.17 μM). However, to our disappointment, their hydroxy analogs **II-4** (clogP=6.59) and **II-5** (clogP=7.67) displayed poor cytotoxicity in the same assay system which might be due to their lower cellular uptake. The highest binding affinity was observed with compound **II-9OH**, exhibiting binding affinity value of 1.64 μM very close to that of tamoxifen (1.42 μM). Among all the active compounds, **II-9OH** also showed maximum inhibition of cell growth against MCF-7 cells with an $IC_{50}$ of 0.81 μM, almost 20 and 16 fold more potent than tamoxifen (15.46 μM) and

raloxifene (13.18 μM), respectively.

2.2.2. Antiangiogenic activity on VEGFR-2 enzyme and HUVEC cells

All the synthesized 2, 4-disubstituted pyrimidine derivatives **I-1**~**I-9**, **II-1**~**II-9**, **II-4OH**, **II-5OH** and **II-9OH** were next evaluated for their enzymatic activities against VEGFR-2 and anti-proliferative activity towards VEGFR-2 overexpressed human umbilical vein endothelial cells (HUVEC). The approved VEGFR-2 inhibitor drug sunitinib was used as a positive control. As shown in Table 2, most of the tested compounds exhibited moderate VEGFR-2 inhibitory activities with more than 50% inhibition at 10 μM. Among these compounds, compound **II-5** which displayed the most potent inhibitory activity against VEGFR-2 with $IC_{50}$ of 0.067 μM was also the most potent one against HUVEC with the $IC_{50}$ of 4.34 μM. While compound **II-9OH** which showed the best binding affinity in previous ERα assay retained promising antiangiogenic activity on both VEGFR-2 enzyme ($IC_{50}$= 0.085 μM) and HUVEC cells ($IC_{50}$= 4.57 μM) compared with sunitinib ($IC_{50}$= 0.054 μM and 4.57 μM, respectively) indicating that **II-9OH** is a potent dual ERα/VEGFR-2 inhibitor.

Most of these compounds demonstrated moderate to good anti-proliferative activities. Compounds **I-3**, **I-4**, **II-5**, **II-6** and **II-9OH** showed better activities against HUVEC cells than the reference drug sunitinib. A close observation of the data showed that the 4-N-linked compounds were more active than their 4-O-linked counterpart (**I-4**~**I-6** vs **I-7**~**I-9** and **II-5**~**II-6** vs **II-8**~**II-9**). It is worthy to note that compounds **I-3**, **I-4** and **II-6** which were less active in VEGFR-2 assay also showed noteworthy inhibition on HUVEC proliferation indicating another mechanism for their acquired activity. On the contrary, **II-3** showing promising activity against VEGFR-2 from the cell-free enzyme assay ($IC_{50}$= 0.203 μM) was not active in HUVEC, which might due to its poor membrane permeability (ClogP = 6.9). Such discrepancies between the inhibitory activity toward HUVEC proliferation and VEGFR-2 inhibition concluded in this manuscript implied that other modes of action or other parameters such as: physicochemical property, cell membrane permeability or target activity could have a significant role in the antiproliferative activity of our novel compounds.

**Table 2**

VEGFR-2 inhibition and antiproliferation activity against HUVEC of all the designed compounds

| Cmpd | VEGFR-2 inhibition | | Antiproliferation ($IC_{50}$, μM)[b] |
|---|---|---|---|
| | Inh% at 10 μM | $IC_{50}$ (μM) | HUVEC |
| **I-1** | 66.24±3.32 | >1 | >40 |
| **I-2** | 44.05±4.78 | >1 | 15.04 |
| **I-3** | 61.29±5.79 | >1 | 4.82 |

| | | | |
|---|---|---|---|
| **I-4** | 40.00±2.88 | >1 | 6.31 |
| **I-5** | 89.70±2.50 | 0.174 | 9.24 |
| **I-6** | 51.88±1.65 | >1 | 11.32 |
| **I-7** | 61.25±1.84 | >1 | >40 |
| **I-8** | 79.99±2.53 | >1 | 23.27 |
| **I-9** | 39.84±3.12 | >1 | 15.84 |
| **II-1** | 50.77±1.85 | >1 | 10.35 |
| **II-2** | 40.22±5.46 | >1 | >40 |
| **II-3** | 87.35±2.06 | 0.203 | >40 |
| **II-4** | 50.94±0.57 | >1 | 14.17 |
| **II-5** | 90.27±2.22 | 0.067 | 4.34 |
| **II-6** | 49.38±3.03 | >1 | 5.02 |
| **II-7** | 90.86±2.47 | 0.101 | 11.72 |
| **II-8** | 60.19±1.47 | >1 | 15.09 |
| **II-9** | 75.32±2.15 | >1 | 10.62 |
| **II-4OH** | 68.45±2.03 | >1 | 13.83 |
| **II-5OH** | 76.92±1.89 | >1 | 8.81 |
| **II-9OH** | 91.07±1.45 | 0.085 | 4.57 |
| **Sunitinib** | 92.74±1.96 | 0.054 | 6.36 |

[a]Percentage inhibition of each compound on VEGFR-2 at 10 μM was measured using homogeneous time resolved fluorescence (HTRF) assay, shown as mean ± SD of three experiments. The $IC_{50}$ values are calculated when Inh% at 1μM is >50%.

[b]$IC_{50}$: concentration that inhibits 50% of cell growth

According to above bioassay results, some of the 2, 4-disubstituted pyrimidines analogs especially **I-5**, **II-5** and **II-9OH** were potent dual-profile ligands. We found that compound **II-9OH** exhibited the strongest ERα binding affinity ($IC_{50}$= 1.64 μM) as well as the best cytotoxicity against MCF-7 cells ($IC_{50}$ = 0.81 μM), also was a promising anti-angiogenesis agent ($IC_{50}$= 0.085 μM for VEGFR-2 inhibition; $IC_{50}$= 4.57 μM against HUVEC cells). This synergetic inhibitory effect of **II-9OH** on ERα and VEGFR-2 suggested it as a promising dual-target agent against breast cancer. Thus, **II-9OH** was selected for our further investigation of its multifunctional effects.

2.2.3. Cytostatic activity and antiestrogenic activity of **II-9OH**

To assess the potential of compound **II-9OH** towards breast cancer, their cytostatic potency was additionally tested against human breast cancer cells T47D (ERα+) and MDA-MB-231 (ERα-). Results presented in Fig. 2A indicated that **II-9OH** strongly inhibited proliferation of both estrogen-responsive and -nonresponsive cells in a dose-dependent manner. Compound **II-9OH** exhibited promising antiproliferative activities against T47D and MDA-MB-231 cells with $IC_{50}$ values at 2.73 and 3.81 μM, respectively. As for ER+ and ER-

breast cancer cells, compound **II-9OH** could inhibit their growth on the same degree which also indicated that the antiproliferative activity was acquired not only through ERα but a multi-target effect.

We further adapted quantitative real-time polymerase chain reaction (RT-PCR) in the ER positive MCF-7 cells to investigate antiestrogenic activity of **II-9OH**. It is known that the expression of ERα-regulated target gene progesterone receptor (PgR) is commonly associated with estrogenic or antiestrogenic activity. As shown in Fig. 2B, compound **II-9OH** at the concentration of 0.4 μM in combination with 10 nM E2 dramatically reduced the expression of PgR mRNA induced by E2 (*** P < 0.001 vs. E2 group), indicating that **II-9OH** presented significantly antiestrogenic property.

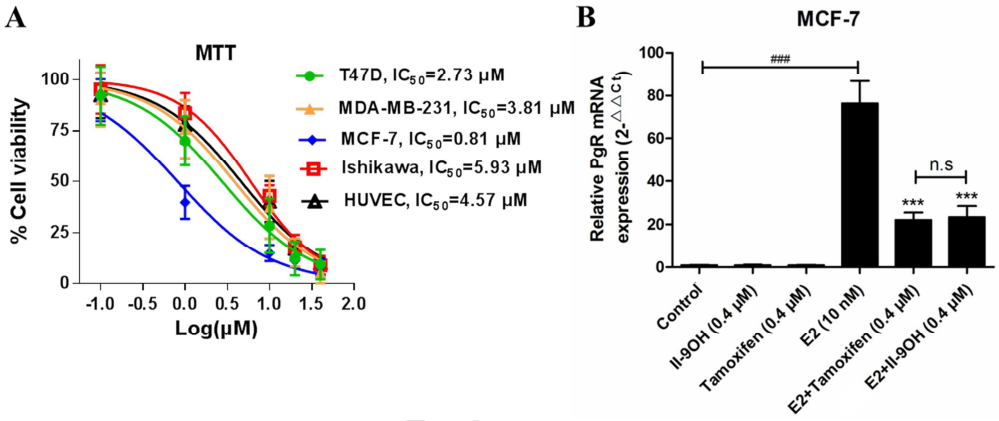


**Figure 2.** (A) *In vitro* anti-proliferative properties of **II-9OH** against T47D and MDA-MB-231 cell lines. (B)The increased mRNA expression of PR induced by E2 was reversed by **II-9OH** in MCF-7 cells. The mRNA expression of PR was examined by Real-time PCR. Values are mean ±SD (n=3). * P < 0.05, ** P < 0.01, *** P < 0.001 vs. E2 group. $^{\#}$ P< 0.05, $^{\#\#}$ P< 0.01, $^{\#\#\#}$ P< 0.001.

2.2.4. **II-9OH** exhibits anti-angiogenic activity *in vivo* and downregulates the protein expression of VEGFR-2 in HUVEC cells

It is well known that vascular endothelial growth factor (VEGF)/VEGFR-2 signaling has a predominant role in angiogenesis, the process of new blood vessel growth from the quiescent pre-existing vessels [30]. Compound **II-9OH** which exhibited potent VEGFR-2 inhibition in enzymatic assay was then selected to evaluate the *in vivo* angiogenetic activity by chick chorioallantoic membrane (CAM) Assay [31]. Compound **II-9OH** dissolved in DMSO were placed on sterile methyl cellulose filter papers at 1 μM, 10 μM and 20 μM with phosphate buffered saline (PBS) as the blank control and sunitinib (1μM) as the positive control. Results are shown in Fig. 3A. Compared with blank control group, compound

**II-9OH** could significantly inhibit angiogenesis in a dose-dependent manner. And the inhibitory activity of compound **II-9OH** was more potent than sunitinib in CAM assay at the same dose (1 μM). Overall, compounds showed potential anti-angiogenesis activities *in vivo*.

The inhibitory effect of compound **II-9OH** on VEGFR-2 was further determined by assessing the phosphorylation level of VEGFR-2 in VEGFR-2 overexpressed HUVEC cells using western blot. As shown in Fig. 3B, **II-9OH** was able to block the phosphorylation of VEGFR-2 significantly compared with control group (*P < 0.05). However, this inhibition effect of **II-9OH** was weaker than that of positive control sunitinib.

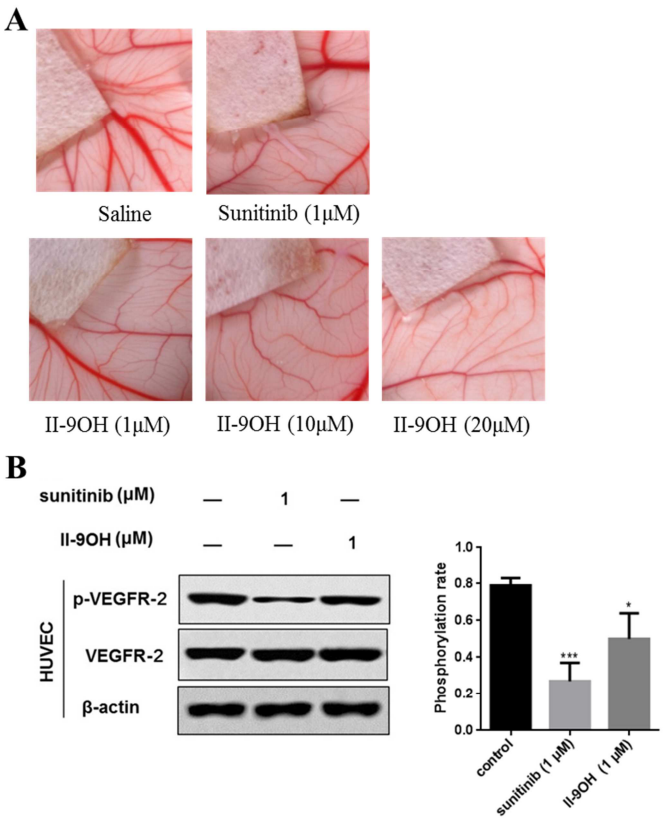


**Figure 3.** (A) *In vivo* Inhibitory effects of compound **II-9OH** on angiogenesis of CAM (B) **II-9OH** inhibits the phosphorylation of VEGFR-2 in HUVEC cells. Expression of p-VEGFR-2 and VEGFR-2 in HUVEC cells were examined by western blots. Densitometric analysis was performed to determine the phosphorylation rate of VEGFR-2. Values are mean ±SD (n=3). * P < 0.05, ** P < 0.01, *** P < 0.001 vs. Control group.

2.2.5. **II-9OH** induces apoptosis and inhibits cancer cell migration in MCF-7 cells through Raf-1/MAPK/ERK signaling inhibition

Because compound **II-9OH** caused a significant reduction in the growth of both ER+ and ER- breast cancer cells, the underlying mechanisms were investigated. First, we measured the induction of apoptosis by this compound using Annexin-V/PI staining and flow cytometry.

Briefly, MCF-7 cells were cultured with 0.5 μM, 1μM of **II-9OH** or 1% DMSO. After incubation for 24 h, cells were subjected to flow cytometric analysis (Fig. 4A). Compound **II-9OH** caused significant induction of apoptosis in a concentration-dependent manner. When treated with 0.5 and 1 μM compound **II-9OH** for 24 h; the percentages of apoptotic cells were 23.39% and 33.49% (Q2 + Q4), respectively, compared with 10.47% of vehicle control.

Metastasis is the major cause of death of the advanced breast cancer patients [32]. Migration of cancer cells is an essential phenomenon exhibited by many types of cancer cells during metastasis. For this assay, a transwell assay was performed to evaluate the ability of MCF-7 cells to pass through the transwell membrane barrier in the presence of **II-9OH**. As shown in Fig. 4B, MCF-7 cells treated with 0.5 μM and 1μM of **II-9OH** showed reduced cell migration as compared to cells treated with vehicle control (DMSO). These results suggested that **II-9OH** played a role in the inhibition of cell migration in breast cancer.

Several cellular signaling pathways are involved in the evolution, aggressiveness and metastatic potential of breast tumors. Currently, studies have revealed that over-expression and aberrant activation of Raf-1/MAPK/ERK pathway is associated with the resistance of endocrine therapy [65]. Crosstalk of estrogen receptor pathway with Raf-1/MAPK/ERK pathway is also relative to breast cancer cell migration, invasion, and angiogenesis [66]. Therefore, we made further investigation of **II-9OH** on inhibiting Raf-1/MAPK/ERK pathway transduction in MCF-7 cells to explore its underlying mechanism of action. Two effectors, Raf-1 and ERK were examined to study how **II-9OH** affected the Raf-1/MAPK/ERK pathway. As expected, the results indicated that 0.5 μM of **II-9OH** significantly inhibited p-Raf-1 and p-ERK1/2 activation, while the total protein level of Raf-1 was not altered (Fig. 4C). To further confirm that the observed transduction inhibition of Raf-1/MAPK/ERK pathway was acquired through VEGFR-2 blockade, a full kinase screening panel is required in further study on mechanism of action.

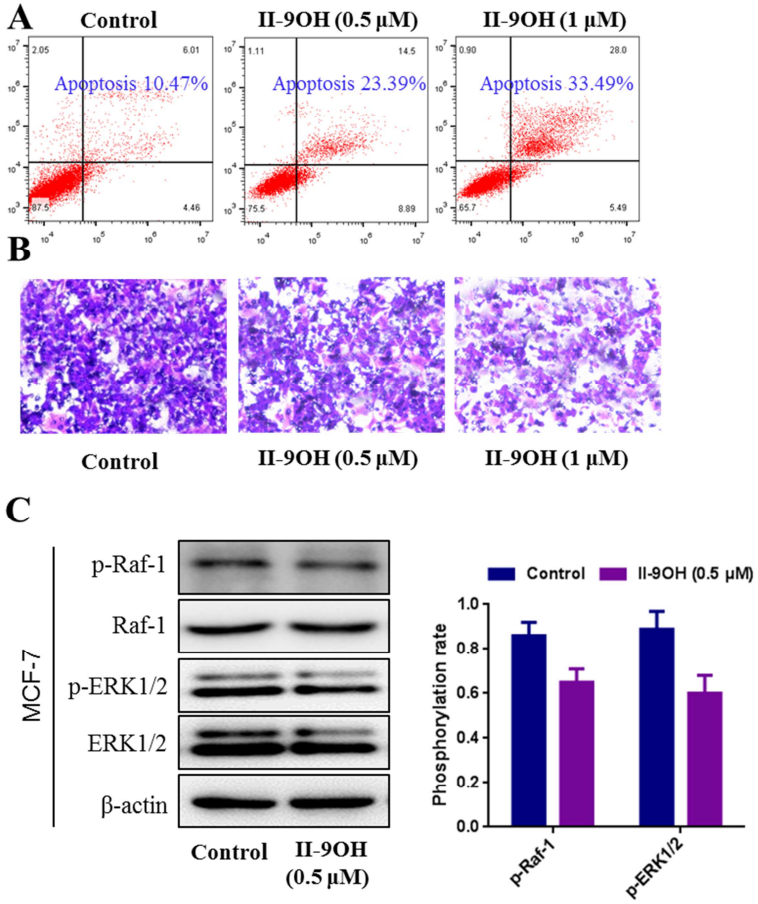


**Figure 4.** (A) Flow cytometry analysis of **II-9OH** on MCF-7 cell apoptosis using Annexin V-FITC/PI. (B) The inhibition of **II-9OH** on MCF-7 cell migration using transwell cell migration assay. (C) Expression of p-Raf-1, Raf-1, p-ERK1/2, and ERK1/2 by 0.5 μM **II-9OH** were examined by western blots in MCF-7 cells. Densitometric analysis was performed to determine the phosphorylation rate of Raf-1 and ERK1/2. Values are mean ± SM (n = 3)

2.3. Molecular docking studies

In order to investigate the possible binding mode of synthesized compounds in ERα/VEGFR-2, molecular docking studies on the potent compound **II-9OH** were performed using the Discovery Studio 3.0/CDOCKER protocol. As shown in Fig. 5A, in the binding pocket of ERα, the pyrimidine scaffold of **II-9OH** is favorably located into the ligand binding domain and the side chain stretches toward the edge of the pocket. Furthermore, an excellent superimposition of **II-9OH** over the structure of 4-hydroxytamoxifen (OHT, co-crystallized ligand) was observed indicating that the designed compounds exhibit the same binding patterns as that of OHT. Detailed docking analysis revealed that that hydroxyl group at C-4' position of 2-phenyl substituent formed hydrogen bonding interactions with Glu353 and Arg394, which is basic requirements for high-affinity ligand binding to ERα (Fig. 5B) [33].

Further docking study of **II-9OH** with VEGFR-2 kinase (PDB ID: 3CJF) confirmed its

predicted mode of binding within the ATP site of VEGFR-2 LBD, with the pyrimidine N-1 making hydrogen acceptor bond with essential amino acid Asn921 (Fig. 6) [22]. Moreover, hydroxyl group at C-4' position of 2-phenyl substituent formed another hydrogen bonding interaction with Asn1031, providing further stabilization for the ligand-receptor complex. These docking results provide additional insights into the protein-ligand interactions and potential structural modifications for further activity improvement.

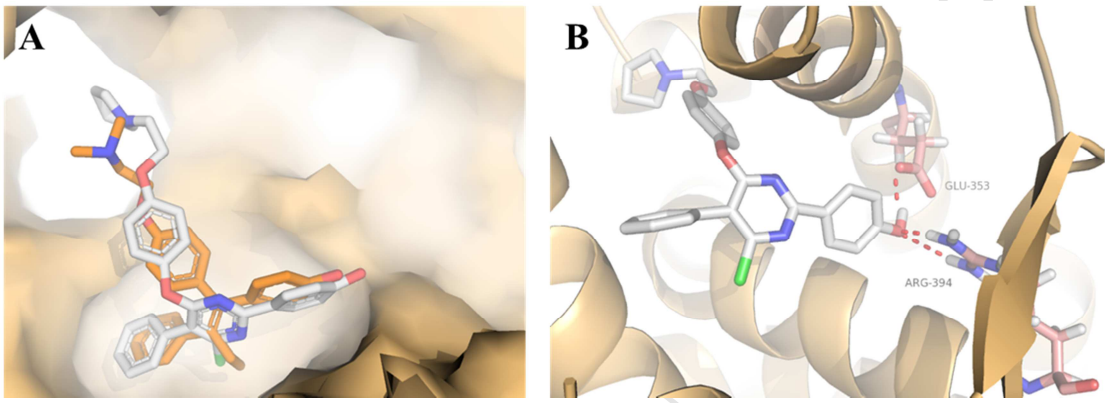


**Figure 5.** (A) Superimposed poses of OHT (orange) with designed compound **II-9OH** (white), binding to ERα (PDB ID: 3ERT), the protein was shown in surface. (B) Docking interactions of **II-9OH** within ERα active site. Dotted lines (red) represent the hydrogen bonding interaction.

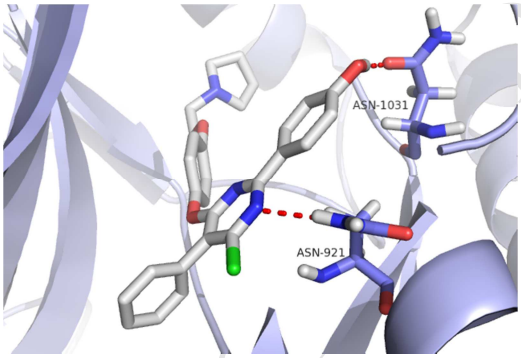


**Figure 6.** Docking poses of **II-9OH** (white) within ATP site of VEGFR-2 (PDB ID: 3CJF). Dotted lines (red) represent the hydrogen bonding interaction.

## 3. Conclusion

To explore different scaffold structures as dual ligands of ERα and VEGFR-2, we have designed and synthesized a series of 2, 4-disubstituted pyrimidines derivatives with basic side chain. Most of them not only exhibited potent ERα binding affinities and VEGFR-2 inhibition, but also showed promising anti-proliferative activities against both cancer cells and angiogenesis-related cells *in vitro*. Among them, Compound **II-9OH** was found to be the most potential inhibitor on the both targets. Further mechanism investigation revealed that

**II-9OH** was able to induce apoptosis and suppress migration in MCF-7 cells by inhibiting signaling transduction of Raf-1/MAPK/ERK pathway. Moreover, **II-9OH** significantly inhibited blood vessel growth in CAM and inhibited the protein expression of VEGFR-2. Collectively, our results demonstrated that the newly developed pyrimidine analogue **II-9OH** showed significant anti-breast cancer efficacy as well as antiangiogenesis activity via a multiple inhibition on ERα/VEGFR-2 and has the potential to be further developed into a promising anti-breast cancer agent.

## 4. Experimental section

### 4.1. Chemistry

#### 4.1.1. General.

Reactions were monitored by thin-layer chromatography (TLC) using precoated silica gel plates (silica gel GF/UV 254), and spots were visualized under UV light (254 nm). Melting points (uncorrected) were determined on a Mel-TEMP II melting point apparatus and are uncorrected. Infrared (IR) spectra (KBr) were recorded on a Nicolet Impact 410 instrument (KBr pellet). $^{1}$H NMR and $^{13}$C NMR spectra were recorded with a Bruker Avance 300 MHz spectrometer at 300 K, using TMS as an internal standard. MS spectra were recorded on a Shimadzu GC-MS 2050 (ESI) or an Agilent 1946A-MSD (ESI) Mass Spectrum. Column chromatography was performed with silica gel (200-300 mesh). Chemical shifts (d) are expressed in parts per million relative to tetramethylsilane, which was used as an internal standard, coupling constants (J) are in hertz (Hz), and the signals are designated as follows: s, singlet; d, doublet; t, triplet; m, multiplet.

#### 4.1.2. Synthesis of 4-methoxybenzonitrile **2**

To a solution of hydroxylammonium chloride (2.57 g, 37 mmol) in 25 ml DMSO was added 4-anisaldehyde (2.27 mL, 20 mmol). The reaction mixture was stirred under reflux for 0.5 h. The resulting mixture was cooled, and the precipitate was collected by filtration, washed with diethyl ether, and then dried in vacuum to obtain **2** as a yellow solid (2.1 g, 78.9%), MS (ESI) m/z: 134.1 ($[M+H]^{+}$).

#### 4.1.3. Synthesis of 4-methoxy-benzamidine hydrochloride **3**

A solution of 4-methoxybenzonitrile **2** (2.1 g, 15.7 mmol), sodium methylate (86 mg, 1.57 mmol) in 20 mL of anhydrous methanol was stirred at room temperature for 48 h. Then ammonium chloride (0.84 g, 15.7mmol) was added, and the reaction group was stirred for

another 24 h. the precipitate was collected by filtration, washed with diethyl ether, and then dried in vacuum to obtain **3** as a white solid (1.3 g, 44.5%), MS (ESI) m/z: 151.1 ($[M+H]^+$).

4.1.4. Synthesis of 2-(4-methoxyphenyl)pyrimidine-4,6-diol **5a**

To a solution of 4-methoxy-benzamidine hydrochloride (0.46 g, 2.47 mmol) in 10 ml anhydrous methanol was added malonate (0.28 mL, 2.47 mmol). A solution of sodium methylate dissolved in 5 ml anhydrous methanol was added to the previous reaction mixture dropwise, and then the reaction mixture was stirred under reflux for 4 h. After the reaction was completed, the resulting mixture was cooled, poured to 50 ml ice water and was dropped by 1 M HCl to pH=4. The precipitate was collected by filtration as a white solid (0.24 g, 45%), MS (ESI) m/z: 217.1 ($[M-H]^-$).

4.1.5. Synthesis of 2-(4-methoxyphenyl)-5-phenylpyrimidine-4,6-diol **5b**

To a solution of 4-methoxy-benzamidine hydrochloride (0.46 g, 2.47 mmol) in 10 ml anhydrous methanol was added malonate (0.53 mL, 2.47 mmol). A solution of sodium methylate dissolved in 5 ml anhydrous methanol was added to the previous reaction mixture dropwise, and then the reaction mixture was stirred under reflux for 4 h. After the reaction was completed, the resulting mixture was cooled, poured to 50 ml ice water and was dropped by 1 M HCl to pH=4. The precipitate was collected by filtration as a white solid (0.3 g, 41%), MS (ESI) m/z: 295.1 ($[M+H]^+$).

4.1.6. Synthesis of 4,6-dichloro-2-(4-methoxyphenyl)pyrimidine **6a**

A solution of 2-(4-methoxyphenyl)pyrimidine-4,6-diol **5a** (1.8 g, 8.24 mmol) in 4 ml phosphorus oxychloride was stirred at 110°C for 5 h. When the reaction was completed, the resulting mixture was cooled, poured to 50 ml ice water and then extracted with ethyl acetate. The organic phase was collected, dried with $Na_2SO_4$ and evaporated to get crude product which was then purified by column chromatograph to give **6a** as a white solid (1.5 g, 71%), MS (ESI) m/z: 256.1 ($[M+H]^+$).

4.1.7. Synthesis of 4,6-dichloro-2-(4-methoxyphenyl)-5-phenylpyrimidine **6b**

Compound **6b** was synthesized from 2-(4-methoxyphenyl)-5-phenylpyrimidine-4,6-diol **5b** (1.7 g, 5.78 mmol) according to the synthetic procedure of **6a** in a yield of 68%, 1.3g. MS (ESI) m/z: 331.1 ($[M+H]^+$).

4.1.8. General synthesis of final compounds **I-1**~**I-6** and **II-1**~**II-6**

A mixture of intermediate **6a** or **6b** (1 equiv), various 4-acetamidoanilines or 4-thoxyanilines (1.5 equiv.), $K_2CO_3$ (2.0 equiv.) and $Pd(PPh_3)_2Cl_2$ in anhydrous dioxane (5.0 mL) was stirred at 100 °C for 8 h. After completion of the reaction as indicated by TLC, the mixture was cooled to room temperature and then extracted, evaporated and purified by flash column chromatography ($CH_2Cl_2$/$CH_3OH$) on silica gel to afford the corresponding pure products **I-1**~**I-6** and **II-1**~**II-6**.

*4.1.9.*

*N-(4-((6-chloro-2-(4-methoxyphenyl)pyrimidin-4-yl)amino)phenyl)-2-(dimethylamino)acetamide* ***I-1***

Yellow solid (0.12g, 34.0%). Mp 118-120 $^oC$; IR (KBr): 3295, 3173, 3077, 2931, 2809, 1663, 1562, 1508, 1372, 1253, 1095, 985, 833 cm-1; $^1$H-NMR (300MHz, $CDCl_3$): δ (ppm) 9.37 (s, 1H, CONH), 8.34-8.37 (d, 2H, 2-Ar-2'-H, *J*=8.97Hz), 7.65-7.68 (d, 2H, 4-Ar-3'-H, *J*=8.73Hz), 7.36-7.39 (d, 2H, 4-Ar-2'-H, *J*=8.82Hz), 6.97-7.00 (d, 2H, 2-Ar-3'-H, *J*=8.94Hz), 6.86 (s, 1H, 5-Ar-H), 6.48 (s, 1H, NH), 3.89 (s, 3H, $OCH_3$), 3.12 (s, 2H, $COCH_2$), 2.35 (S, 6H). $^{13}$C NMR (75 MHz, $CDCl_3$): δ 170.3, 164.7, 162.1, 160.6, 134.5, 134.1, 130.4, 129.3, 123.6, 120.5, 113.8, 100.1, 57.5, 53.6, 44.5. MS (ESI, m/z): 412.2$[M+H]^+$.

*4.1.10.*

*N-(4-((6-chloro-2-(4-methoxyphenyl)pyrimidin-4-yl)amino)phenyl)-2-(diethylamino)acetamide* ***I-2***

Yellow solid (0.13 g, 37.9%). Mp 127-128$^oC$; IR (KBr): 3316, 3153, 3076, 2964, 2818, 1656, 1561, 1508, 1373, 1253, 1096, 985, 835 $cm^{-1}$; $^1$H-NMR (300MHz, $CDCl_3$): δ (ppm) 9.51 (s, 1H, CONH), 8.34-8.36 (d, 2H, 2-Ar-2'-H, *J*=8.79Hz), 7.65-7.71 (d, 2H, 4-Ar-3'-H, *J*=8.67Hz), 7.35-7.38 (d, 2H, 4-Ar-2'-H, *J*=8.58Hz), 6.96-6.99 (d, 2H, 2-Ar-3'-H, *J*=8.88Hz), 6.90 (s, 1H, 5-Ar-H), 6.48 (s, 1H, NH), 3.89 (s, 3H, $OCH_3$), 3.18 (s, 2H, $COCH_2$ ), 2.64-2.72 (q, 4H, $NCH_2$, J=7.05Hz), 1.10-1.15 (t, 6H, $NCH_2CH_3$, *J*=7.11Hz). $^{13}$C NMR (75 MHz, $CDCl_3$): δ 170.4, 164.6, 162.1, 160.5, 134.8, 133.9, 130.1, 129.3, 123.5, 120.5, 113.7, 100.1, 58.0, 55.4, 48.9, 12.5. MS (ESI) m/z: 440.3 $[M+H]^+$, 462.3$[M+Na]^+$.

*4.1.11.*

*N-(4-((6-chloro-2-(4-methoxyphenyl)pyrimidin-4-yl)amino)phenyl)-2-(pyrrolidin-1-yl)acetamide* ***I-3***

Yellow solid (98 mg, 28.6%). Mp 208-210°C; IR (KBr): 3447, 3304, 3211, 2953, 2812, 1676, 1560, 1511, 1370, 1244, 1096, 984, 825 $cm^{-1}$; $^1$H-NMR (300MHz, DMSO): δ (ppm) 9.81 (s, 1H, CONH), 9.72 (s, 1H, 5-Ar-H), 8.22-8.24 (d, 2H, 2-Ar-2'-H, *J*=8.76Hz), 7.63-7.69 (m, 4H, 4-Ar-H), 7.06-7.09 (d, 2H, 2-Ar-3'-H, *J*=8.79Hz), 6.60 (s, 1H, NH), 3.83 (s, 3H, $OCH_3$), 3.23 (s, 2H, $COCH_2$), 2.58 (brs, 4H, 2, 5-pyrrolidyl-H), 1.74 (brs, 4H, 3, 4-pyrrolidyl-H). $^{13}$C NMR (75 MHz, $CDCl_3$): δ 170.5, 164.7, 162.1, 160.5, 134.9, 133.9, 130.1, 129.4, 123.6, 120.5, 113.8, 100.0, 58.1, 55.5, 49.9, 23.8. MS (ESI, m/z): 438.3$[M+H]^+$.

*4.1.12.*

*6-chloro-N-(4-(2-(dimethylamino)ethoxy)phenyl)-2-(4-methoxyphenyl)pyrimidin-4-amine* ***I-4***

Yellow solid (98 mg, 31.5%). Mp 113-116°C; IR (KBr): 3447, 2933, 2822, 2777, 1593, 1569, 1507, 1397, 1247, 1166, 1208, 844 $cm^{-1}$; $^1$H-NMR (300MHz, $CDCl_3$): δ (ppm) 8.32-8.35 (d, 2H, 2-Ar-2'-H, *J*=8.82Hz), 7.23-7.26 (d, 2H, 4-Ar-2'-H, *J*=8.58Hz), 6.93-6.98 (m, 5H, 4-Ar-3'-H, 2-Ar-3'-H, 5-Ar-H), 6.37 (s, 1H, NH), 4.08-4.12 (t, 2H, $OCH_2CH_2$, *J*=5.52Hz), 3.88 (s, 3H, $OCH_3$), 2.75-2.79 (t, 2H, $OCH_2CH_2$, *J*=5.46Hz), 2.37 (s, 6H, $N(CH_3)_2$). $^{13}$C NMR (75 MHz, $CDCl_3$): δ 163.6, 162.8, 162.3, 162.1, 161.2, 155.8, 132.4, 131.4, 130.1, 129.5, 125.6, 124.9, 115.5, 115.2, 113.7, 113.4, 66.2, 58.3, 55.3, 45.9, 37.1. MS (ESI, m/z): 397.2$[M-H]^-$.

*4.1.13.*

*6-chloro-N-(4-(2-(diethylamino)ethoxy)phenyl)-2-(4-methoxyphenyl)pyrimidin-4-amine* ***I-5***

Yellow solid (0.12 g, 36.0%). Mp 122-124°C; IR (KBr): 2975, 2930, 2811, 1585, 1565, 1507, 1389, 1304, 1235, 1168, 1028, 820 $cm^{-1}$; $^1$H-NMR (300MHz, $CDCl_3$): δ (ppm) 8.32-8.35 (d, 2H, 2-Ar-2'-H, *J*=7.59Hz), 7.22-7.26 (d, 2H, 4-Ar-2'-H), 6.95-6.97 (m, 4H, 4-Ar-3'-H, 2-Ar-3'-H), 6.79 (s, 1H, 5-Ar-H), 6.36 (s, 1H, NH), 4.07 (t, 2H, $OCH_2CH_2$), 3.88 (s, 3H, $OCH_3$), 2.90 (t, 2H, $OCH_2CH_2$), 2.63-2.67 (q, 4H, $N(CH_2CH_3)_2$, *J*=6.66Hz), 1.07-1.11 (t, 6H, $N(CH_2CH_3)_2$, *J*=6.39Hz ). $^{13}$C NMR (75 MHz, $CDCl_3$): δ 164.6, 162.9, 162.1, 160.6, 157.0, 130.1, 130.1, 129.3, 125.7, 115.4, 113.7, 99.2, 66.9, 55.4, 51.7, 47.8, 11.8. MS (ESI, m/z): 427.2$[M+H]^+$.

*4.1.14.*

*6-chloro-2-(4-methoxyphenyl)-N-(4-(2-(pyrrolidin-1-yl)ethoxy)phenyl)pyrimidin-4-amine* ***I-6***

Yellow solid (0.13 g, 39.2%). Mp 140-142°C; IR (KBr): 3421, 2970, 2933, 2804, 1592, 1568, 1508, 1395, 1246, 1161, 1035, 840 $cm^{-1}$; $^1$H-NMR (300MHz, CDCl3): δ (ppm) 8.34-8.36 (d,

2H, 2-Ar-2'-H, *J*=7.26Hz), 7.23-7.26 (d, 2H, 4-Ar-2'-H), 6.92-6.96 (m, 4H, 4-Ar-3'-H, 2-Ar-3'-H), 6.77 (s, 1H, 5-Ar-H), 6.36 (s, 1H, NH), 4.12 (brs, 2H, $OCH_2CH_2$), 3.87 (s, 3H, $OCH_3$), 2.92 (brs, 2H, $OCH_2CH_2$), 2.64 (brs, 4H, 2, 5-pyrrolidyl-H), 1.60 (brs, 4H, 3, 4-pyrrolidyl-H). $^{13}$C NMR (75 MHz, $CDCl_3$): δ 164.7, 162.9, 162.3, 160.7, 157.0, 130.1, 130.0, 129.0, 125.8, 115.4, 113.7, 99.1, 67.0, 55.4, 51.8, 48.9, 24.1. MS (ESI, m/z): 423.1$[M-H]^-$.

*4.1.15.*

*N-(4-((6-chloro-2-(4-methoxyphenyl)-5-phenylpyrimidin-4-yl)amino)phenyl)-2-(dimethylamino)acetamide* ***II-1***

Yellow solid (145 mg, 50%). Mp 171-173°C; IR (KBr): 3410, 3297, 2942, 2835, 2787, 1675, 1550, 1513, 1404, 1246, 1173, 844, 789 $cm^{-1}$; $^1$H-NMR (300MHz, CDCl3): δ (ppm) 9.15 (s, 1H, CONH), 8.37-8.39 (d, 2H, 2-Ar-2'-H, *J*=6.99Hz), 7.55-7.60 (m, 7H, 5-Ar-H, 4-Ar-3'-H), 7.44 (d, 2H, 4-Ar-2'-H), 6.98-7.00 (d, 2H, 2-Ar-3'-H, *J*=6.24Hz), 6.45 (s, 1H, NH), 3.89 (s, 3H, $OCH_3$), 3.09 (s, 2H, CH*2*), 2.39 (s, 6H, $N(CH_3)_2$). $^{13}$C NMR (75 MHz, DMSO): δ 170.0, 162.1, 161.8, 160.0, 158.0, 134.8, 134.8, 132.7, 130.8, 129.9, 129.7, 129.2, 129.1, 123.7, 119.5, 115.4, 114.5, 57.9, 55.6, 45.3. MS (ESI, m/z): 488.3 $[M+H]^+$.

*4.1.16.*

*N-(4-((6-chloro-2-(4-methoxyphenyl)-5-phenylpyrimidin-4-yl)amino)phenyl)-2-(diethylamino) acetamide* ***II-2***

Yellow solid (150 mg, 49.7%). Mp 131-132°C; IR (KBr): 3409, 3299, 3970, 2934, 2824, 1682, 1545, 1514, 1405, 1250, 1173, 842, 791 $cm^{-1}$; $^1$H-NMR (300MHz, $CDCl_3$): δ (ppm) 9.43 (s, 1H, CONH), 8.37-8.39 (d, 2H, 2-Ar-2'-H, *J*=7.11Hz), 7.52-7.61 (m, 7H, 5-Ar-H, 4-Ar-3'-H), 7.42-7.44 (d, 2H, 4-Ar-2'-H, *J*=6.78Hz), 6.98-7.00 (d, 2H, 2-Ar-3'-H, *J*=7.02Hz), 6.45 (s, 1H, NH), 3.89 (s, 3H, $OCH_3$), 3.15 (s, 2H, $COCH_2$), 2.62-2.69 (q, 4H, $NCH_2$, *J*=6.84Hz), 1.08-1.12(t, 6H, $CH_2CH_3$, *J*=7.05Hz). $^{13}$C NMR (75 MHz, DMSO): δ 170.1, 162.2, 161.8, 159.9, 157.9, 134.8, 134.8, 132.8, 130.8, 129.9, 129.7, 129.3, 129.2, 123.7, 119.5, 115.3, 114.5, 57.8, 55.8, 48.3, 12.4. MS (ESI, m/z): 516.2$[M+H]^+$.

*4.1.17.*

*N-(4-((6-chloro-2-(4-methoxyphenyl)-5-phenylpyrimidin-4-yl)amino)phenyl)-2-(pyrrolidin-1-yl)acetamide* ***II-3***

Yellow solid (110 mg, 35.7%). Mp 162-165°C; IR (KBr): 3408, 3290, 2939, 2813, 1678, 1547,

1516, 1405, 1250, 1170, 842, 790 $cm^{-1}$; $^{1}$H-NMR (300MHz, $CDCl_3$): δ (ppm) 9.30 (s, 1H, CONH), 8.37-8.39 (d, 2H, 2-Ar-2'-H, *J*=6.93Hz), 7.52-7.61 (m, 7H, 5-Ar-H, 4-Ar-3'-H), 7.42-7.44 (d, 2H, 4-Ar-2'-H, *J*=6.6Hz), 6.98-7.00 (d, 2H, 2-Ar-3'-H, *J*=7.05Hz), 6.45 (s, 1H, NH), 3.89 (s, 3H, $OCH_3$), 3.08 (s, 2H, $COCH_2$), 2.56 (brs, 4H, 2,5-pyrrolidyl-H), 1.66 (brs, 4H, 3, 4-pyrrolidyl-H). $^{13}$C NMR (75 MHz, DMSO): δ 168.8, 162.1, 161.8, 159.9, 157.99, 134.9, 134.7, 132.8, 130.8, 129.9, 129.7, 129.3, 129.2, 123.7, 119.6, 115.3, 114.4, 63.1, 55.8, 54.6, 25.9, 23.9. MS (ESI, m/z): 514.3$[M+H]^+$.

*4.1.18.*

*6-chloro-N-(4-(2-(dimethylamino)ethoxy)phenyl)-2-(4-methoxyphenyl)-5-phenylpyrimidin-4-amine* ***II-4***

Yellow solid (93 mg, 32.6%). Mp 68-70°C; IR (KBr): 3621, 3417, 3321, 2940, 2831, 1601, 1573, 1540, 1408, 1254, 1168, 1029, 795 $cm^{-1}$; $^{1}$H-NMR (300MHz, $CDCl_3$): δ (ppm) 8.34-8.36 (d, 2H, 2-Ar-2'-H, *J*=6.81Hz), 7.42-7.57 (m, 7H, 5-Ar-H, 4-Ar-2'-H), 6.91-6.98 (m, 4H, 2-Ar-3'-H, 4-Ar-3'-H), 6.36 (s, 1H, NH), 4.07 (brs, 2H, $OCH_2$), 3.88 (s, 3H, $OCH_3$), 2.73 (brs, 2H, $OCH_2CH_2N$), 2.35(s, 6H, $N(CH_3)_2$). $^{13}$C NMR (75 MHz, $CDCl_3$): δ 162.8, 162.0, 159.3, 157.8, 155.5, 132.6, 131.6, 130.2, 130.1, 129.7, 129.6, 129.2, 122.9, 114.7, 114.5, 113.7, 66.3, 58.3, 55.4, 45.9. MS (ESI, m/z): 475.2$[M+H]^+$.

*4.1.19.*

*6-chloro-N-(4-(2-(diethylamino)ethoxy)phenyl)-2-(4-methoxyphenyl)-5-phenylpyrimidin-4-amine* ***II-5***

Yellow solid (120 mg, 39.8%). Mp 47-49°C; IR (KBr): 3620, 3413, 3287, 2977, 2838, 1601, 1571, 1540, 1407, 1259, 1166, 1029, 979, 795 $cm^{-1}$; $^{1}$H-NMR (300MHz, $CDCl_3$) : δ (ppm) 8.34-8.36 (d, 2H, 2-Ar-2'-H, J=7.17Hz), 7.41-7.58 (m, 7H, 5-Ar-H, 4-Ar-2'-H), 6.96-6.98 (d, 2H, 2-Ar-3'-H, *J*=7.53), 6.89-6.92 (d, 2H, 4-Ar-3'-H, *J*=7.95), 6.38 (s, 1H, NH), 4.06 (t, 2H, OCH2, *J*=5.27Hz), 3.88 (s, 3H, $OCH_3$), 2.89 (t, 2H, $OCH_2CH_2N$, *J*=5.37Hz), 2.63-2.67 (m, 4H, $NCH_2CH_3$), 1.06-1.10 (t, 6H, $NCH_2CH_3$, *J*=6.57Hz). $^{13}$C NMR (75 MHz, $CDCl_3$): δ 162.8, 162.0, 159.3, 157.8, 155.5, 132.6, 131.5, 130.2, 130.1, 129.7, 129.6, 129.2, 122.9, 114.6, 114.5, 113.7, 66.8, 55.4, 51.7, 47.8, 11.8. MS (ESI, m/z): 503.2$[M+H]^+$.

*4.1.20.*

*6-chloro-2-(4-methoxyphenyl)-5-phenyl-N-(4-(2-(pyrrolidin-1-yl)ethoxy)phenyl)pyrimidin-4-amine* ***II-6***

Yellow solid (98 mg, 32.7%) Mp 87-89°C; IR (KBr): 3611, 3418, 3343, 2965, 2826, 1600, 1573, 1539, 1407, 1256, 1167, 1026, 981, 795 $cm^{-1}$; $^1$H-NMR (300MHz, $CDCl_3$): δ (ppm) 8.34-8.36 (d, 2H, 2-Ar-2'-H, *J*=7.08Hz), 7.42-7.57 (m, 7H, 5-Ar-H, 4-Ar-2'-H), 6.90-6.98 (m, 4H, 2-Ar-3'-H, 4-Ar-3'-H), 6.36 (s, 1H, NH), 4.11 (brs, 2H, $OCH_2$), 3.88 (s, 3H, $OCH_3$), 2.91 (brs, 2H, $OCH_2CH_2N$), 2.63 (brs, 4H, 2, 5-pyrrolidyl-H), 1.82 (brs, 4H, 3, 4-pyrrolidyl-H). $^{13}$C NMR (75 MHz, $CDCl_3$): δ 162.8, 162.0, 159.3, 157.8, 155.6, 132.6, 131.4, 130.2, 130.0, 129.7, 129.6, 129.2, 122.8, 114.6, 114.5, 113.7, 66.9, 55.4, 51.7, 47.8, 23.5.MS (ESI, m/z): 501.2$[M+H]^+$.

*4.1.21. General synthesis of final compounds **I-7~I-9** and **II-7~II-9***

A mixture of intermediate **6a** or **6b** (1 equiv), various 4-acetamidophenoxy or 4-thoxyphenoxy (1.0 equiv) and $K_2CO_3$ (1.0 equiv.) in anhydrous DMF (8.0 mL) was stirred at 80 °C for 4 h. After completion of the reaction as indicated by TLC, the mixture was cooled to room temperature and then extracted, evaporated and purified by flash column chromatography ($CH_2Cl_2$/$CH_3OH$) on silica gel to afford the corresponding pure products **I-7~I-9** and **II-7~II-9**.

*4.2.22.*

*2-(4-((6-chloro-2-(4-methoxyphenyl)pyrimidin-4-yl)oxy)phenoxy)-N,N-dimethylethanamine* ***I-7***

Yellow solid (83 mg, 26.6%). $^1$H-NMR (300MHz, $CDCl_3$): δ (ppm) 8.24-8.27 (dd, 2H, 2-Ar-2'-H, *J*=6.99Hz, *J*=1.95Hz), 7.11-7.14 (dd, 2H, 4-Ar-2'-H, *J*=6.81Hz, *J*=2.28Hz), 6.98-7.01 (dd, 2H, 4-Ar-3'-H, *J*=6.84Hz, *J*=2.28Hz), 6.91-6.94 (dd, 2H, 2-Ar-3'-H, *J*=7.08Hz, *J*=1.92Hz), 6.61 (s, 1H, 5-Ar-H), 4.09-4.13 (t, 2H, $OCH_2CH_2N$, *J*=5.67Hz), 3.87 (s, 3H, $OCH_3$), 2.76-2.80 (t, 2H, $OCH_2CH_2N$, *J*=5.64Hz), 2.38 (s, 6H, $N(CH_3)_2$). δ 170.8, 164.9, 162.4, 161.9, 156.7, 145.7, 130.4, 128.2, 122.6, 115.4, 113.7, 103.6, 66.5, 57.9, 55.3, 55.1. MS (ESI, m/z): 400.1$[M+H]^+$.

*4.2.23.*

*2-(4-((6-chloro-2-(4-methoxyphenyl)pyrimidin-4-yl)oxy)phenoxy)-N,N-diethylethanamine* ***I-8***

Yellow solid (0.187 g, 56.0%). Mp 59-61°C; IR (KBr): 3448, 3113, 2965, 2934, 2785, 1664, 1607, 1541, 1503, 1253, 1198, 1036, 962 $cm^{-1}$; $^1$H-NMR (300MHz, $CDCl_3$): δ (ppm) 8.24-8.27 (d, 2H, 2-Ar-2'-H, *J*=8.73Hz), 7.10-7.13 (d, 2H, 4-Ar-2'-H, *J*=8.88Hz), 6.91-6.99 (m, 4H, 4-Ar-3'-H, 2-Ar-3'-H), 6.60 (s, 1H, 5-Ar-H), 4.07-4.11 (t, 2H, $OCH_2CH_2N$,

*J*=6.15Hz), 3.86 (s, 3H, $OCH_3$), 2.89-2.93 (t, 2H, $OCH_2CH_2N$, *J*=5.64Hz), 2.64-2.71 (q, 4H, $N(CH_2CH_3)_2$, *J*=7.11Hz), 1.08-1.13 (t, 6H, $N(CH_2CH_3)_2$, *J*=7.11Hz). $^{13}C$ NMR (75 MHz, $CDCl_3$): δ 170.8, 164.8, 162.5, 162.0, 156.6, 145.7, 130.4, 128.4, 122.4, 115.4, 113.8, 103.6, 66.4, 57.9, 55.4, 55.1, 25.9. MS (ESI, m/z): 428.2$[M+H]^+$.

*4.2.24. 4-chloro-2-(4-methoxyphenyl)-6-(4-(2-(pyrrolidin-1-yl)ethoxy)phenoxy)pyrimidine* ***I-9***

Yellow solid (0.167 g, 50.3%). Mp 82-84°C; IR (KBr): 3422, 3073, 2922, 2818, 2786, 1609, 1541, 1502, 1253, 1192, 1087, 964 $cm^{-1}$; $^1H$-NMR (300MHz, $CDCl_3$): δ (ppm) 8.24-8.27 (d, 2H, 2-Ar-2'-H, *J*=8.91Hz), 7.10-7.13 (d, 2H, 4-Ar-2'-H, *J*=9.03Hz), 6.91-7.01 (m, 4H, 4-Ar-3'-H, 2-Ar-3'-H), 6.61 (s, 1H, 5-Ar-H), 4.13-4.17 (t, 2H, $OCH_2CH_2N$, *J*=5.91Hz), 3.86 (s, 3H, $OCH_3$), 2.93-2.97 (t, 2H, $OCH_2CH_2N$, *J*=5.88Hz), 2.66 (brs, 4H, 2, 5-pyrrolidyl-H), 1.84 (brs, 4H, 3, 4-pyrrolidyl-H). $^{13}C$ NMR (75 MHz, $CDCl_3$): δ 170.9, 164.8, 162.4, 162.1, 156.5, 145.8, 130.4, 128.3, 122.4, 115.4, 113.8, 103.7, 66.3, 57.9, 55.5, 46.3, 23.8. MS (ESI, m/z): 426.1$[M+H]^+$.

*4.2.25.*

*2-(4-((6-chloro-2-(4-methoxyphenyl)-5-phenylpyrimidin-4-yl)oxy)phenoxy)-N,N-dimethyletha namine* ***II-7***

Yellow solid (0.273 g, 63.0%). Mp 97-100°C; IR (KBr): 3448, 2932, 2818, 2770, 1601, 1570, 1500, 1406, 1253, 1189, 972, 845 $cm^{-1}$; $^1H$-NMR (300MHz, $CDCl_3$): δ (ppm) 8.17-8.20 (d, 2H, 2-Ar-2'-H, *J*=8.37Hz), 7.48-7.52 (m, 5H, 5-Ar-H), 7.07-7.10 (d, 2H, 4-Ar-2'-H), 6.90-6.98 (m, 4H, 4-Ar-3'-H, 2-Ar-3'-H), 4.09-4.12 (t, 2H, $OCH_2CH_2N$, *J*=5.07Hz), 3.86 (s, 3H, $OCH_3$), 2.76-2.79 (t, 2H, $OCH_2CH_2N$, *J*=4.80Hz), 2.39 (s, 6H, $N(CH_3)_2$). $^{13}C$ NMR (75 MHz, $CDCl_3$): δ 167.6, 162.40, 162.3, 160.2, 156.2, 146.3, 131.8, 130.3, 130.2, 128.5, 128.3, 122.6, 117.8, 114.9, 113.8, 66.4, 58.4, 55.4, 46.0. MS (ESI, m/z): 476.3$[M+H]^+$.

*4.2.26.*

*2-(4-((6-chloro-2-(4-methoxyphenyl)-5-phenylpyrimidin-4-yl)oxy)phenoxy)-N,N-diethylethana mine* ***II-8***

Yellow solid (0.262 g, 57.1%). Mp 93-96°C; IR (KBr): 3447, 2969, 2917, 2848, 1602, 1569, 1498, 1405, 1251, 1188, 1168, 971 $cm^{-1}$; $^1H$-NMR (300MHz, $CDCl_3$): δ (ppm) 8.17-8.20 (d, 2H, 2-Ar-2'-H, *J*=8.82Hz), 7.45-7.52 (m, 5H, 5-Ar-H), 7.07-7.10 (d, 2H, 4-Ar-2'-H, *J*=8.97Hz), 6.90-6.96 (m, 4H, 4-Ar-3'-H, 2-Ar-3'-H), 4.07-4.11 (t, 2H, $OCH_2CH_2N$, *J*=6.15Hz), 3.86 (s, 3H, $OCH_3$), 2.89-2.94 (t, 2H, $OCH_2CH_2N$, *J*=6.18 Hz), 2.65-2.72 (q, 4H,

$N(CH_2CH_3)_2$, *J*=7.11Hz), 1.09-1.13 (t, 6H, $N(CH_2CH_3)_2$, *J*=7.11Hz). $^{13}C$ NMR (75 MHz, $CDCl_3$): δ 167.6, 162.4, 162.3, 160.2, 156.2, 146.3, 131.8, 130.3, 130.2, 128.5, 128.3, 122.6, 117.8, 114.9, 113.8, 67.0, 55.4, 51.8, 47.9, 11.9. MS (ESI, m/z): 504.4$[M+H]^+$.

*4.2.27.*

*4-chloro-2-(4-methoxyphenyl)-5-phenyl-6-(4-(2-(pyrrolidin-1-yl)ethoxy)phenoxy)pyrimidine* ***II-9***

Yellow solid (0.281 g, 61.5%). Mp 121-123°C; IR (KBr): 3448, 2956, 2931, 2812, 1602, 1571, 1500, 1405, 1250, 1192, 1028, 973 $cm^{-1}$; $^1H$-NMR (300MHz, $CDCl_3$): δ (ppm) 8.17-8.20 (d, 2H, 2-Ar-2'-H, *J*=8.76Hz), 7.46-7.52 (m, 5H, 5-Ar-H), 7.06-7.09 (d, 2H, 4-Ar-2'-H, *J*=8.91Hz), 6.90-6.97 (m, 4H, 4-Ar-3'-H, 2-Ar-3'-H), 4.13-4.17 (t, 2H, $OCH_2CH_2N$, *J*=5.82Hz), 3.86 (s, 3H, $OCH_3$), 2.93-2.97 (t, 2H, $OCH_2CH_2N$, *J*=5.79Hz), 2.68 (brs, 4H, 2, 5-pyrrolidyl-H), 1.85 (brs, 4H, 3, 4-pyrrolidyl-H). $^{13}C$ NMR (75 MHz, $CDCl_3$): δ 167.7, 162.4, 162.3, 160.1, 156.2, 146.4, 131.9, 130.2, 130.2, 128.5, 128.3, 122.7, 117.9, 115.0, 113.9, 67.0, 55.4, 51.8, 48.5, 12.1.MS (ESI, m/z): 502.4$[M+H]^+$.

4.2.28. General synthesis of final compounds **II-4OH**, **II-5OH** and **II-9**

A solution of **II-4** or **II-5** or **II-9** (0.23 mmol) in dry $CH_2Cl_2$ (5mL) was cooled to -30°C by cryotrap. A solution of $BBr_3$ (2.4mmol) in dry $CH_2Cl_2$ (2.4mL) was added dropwise under nitrogen. The mixture was gently warmed to room temperature and stirred for 4 h. The reaction mixture was quenched with ice water, then saturated sodium bicarbonate solution was adjusted to pH=8 and further purified by silica gel column chromatography to afford the demethylation products **II-4OH**, **II-5OH** and **II-9**.

*4.2.29.*

*4-(4-chloro-6-((4-(2-(dimethylamino)ethoxy)phenyl)amino)-5-phenylpyrimidin-2-yl)phenol* ***II-4OH***

Yellow solid (62.3%). $^1H$-NMR (300MHz, $CDCl_3$) : δ (ppm) 10.09 (s, 1H, OH), 8.17-8.20 (dd, 2H, 2-Ar-2'-H, *J*=7.05Hz, *J*=1.98Hz), 7.46-7.52 (m, 5H, 5-Ar-H), 7.07-7.10 (dd, 2H, 4-Ar-2'-H, *J*=6.81Hz, *J*=2.19Hz), 6.90-6.96 (m, 4H, 4-Ar-3'-H, 2-Ar-3'-H), 4.13-4.17 (t, 2H, $OCH_2CH_2N$, *J*=5.70Hz), 3.86 (s, 3H, $OCH_3$), 2.73 (brs, 2H, $OCH_2CH_2N$), 2.35(s, 6H, $N(CH_3)_2$).MS (ESI, m/z) : 461.2$[M+H]^+$.

*4.2.30.*

*4-(4-chloro-6-((4-(2-(diethylamino)ethoxy)phenyl)amino)-5-phenylpyrimidin-2-yl)phenol*

***II-5OH***

Yellow solid (54.1%); IR (KBr) : 3178, 2937, 2852, 2792, 1561, 1506, 1380, 1251, 1169, 1035, 823 $cm^{-1}$; $^{1}$H-NMR (300MHz, $CDCl_3$): δ (ppm) 10.15 (s, 1H, OH), 8.16-8.19 (dd, 2H, 2-Ar-2'-H, *J*=6.96Hz, *J*=2.04Hz), 7.46-7.52 (m, 5H, 5-Ar-H), 7.06-7.09 (dd, 2H, 4-Ar-2'-H, *J*=6.81Hz, *J*=2.25Hz), 6.89-6.95 (m, 4H, 4-Ar-3'-H, 2-Ar-3'-H), 4.12-4.16 (t, 2H, $OCH_2CH_2N$, *J*=5.82Hz), 3.85 (s, 3H, $OCH_3$), 2.89 (t, 2H, $OCH_2CH_2N$, *J*=5.37Hz), 2.63-2.67 (m, 4H, $NCH_2CH_3$), 1.06-1.10 (t, 6H, $NCH_2CH_3$, *J*=6.57Hz). MS (ESI, m/z): 490.2$[M+H]^+$.

*4.2.31. 4-(4-chloro-5-phenyl-6-(4-(2-(pyrrolidin-1-yl)ethoxy)phenoxy)pyrimidin-2-yl)phenol*

***II-9OH***

Yellow solid (57 mg, 58.5%). Mp 203-205°C; IR (KBr): 3431, 2919, 2481, 1569, 1499, 1408, 1379, 1236, 1188, 1165, 972 $cm^{-1}$; $^{1}$H-NMR (300MHz, DMSO): δ (ppm) 10.17 (s, 1H, OH), 7.90-7.93 (d, 2H, 2-Ar-2'-H, *J*=8.82Hz), 7.42-7.59 (m, 5H, 5-Ar-H), 7.16-7.19 (d, 2H, 4-Ar-2'-H, *J*=9.06Hz), 6.99-7.02 (d, 2H, 4-Ar-3'-H, J=9.09Hz), 6.80-6.83 (d, 2H, 2-Ar-3'-H, J=8.79Hz), 4.10-4.14 (t, 2H, $OCH_2CH_2N$, *J*=5.79Hz), 2.91 (brs, 2H, $OCH_2CH_2N$), 2.65 (brs, 4H, 2, 5-pyrrolidyl-H), 1.72 (brs, 4H, 3, 4-pyrrolidyl-H). $^{13}$C NMR (75 MHz, DMSO): δ 164.6, 162.9, 162.1, 160.7, 157.0, 130.2, 130.1, 129.3, 125.7, 115.5, 113.7, 99.2, 66.2, 57.9, 55.4, 55.1, 25.9. MS (ESI, m/z): 488.2$[M+H]^+$.

4.2 Biological evaluation

4.2.1. ERα Binding Affinity Assay.

The recombinant ERα (Thermo Fisher Scientific Inc., Invitrogen, USA) and the fluorescent estrogen ligands (self-made) were removed from the -80$^{o}$C freezer and thawed on ice for 1 h prior to use. The fluorescent estrogen ligand was added to the ERα and screening buffer (ES2 Screening Buffer, Invitrogen, USA) was added to make the final concentration 9 nM for fluorescent estrogen and 30 nM for ERα. Test compounds were accurately weighed and dissolved in DMSO, screening buffer was added to dilute to required concentration. Test compound (1 μL) was added to 49 μL screening buffer in each well (384-well microplate, Corning, USA). To this 50 μL of the fluorescent estrogen/ER complex was added to make up a final volume of 100 μL. A positive control contained 50 μL estradiol buffer (1nM) and 50 μL fluorescent estrogen/ER complexes. A negative control contained 50 μL screening buffer and 50 μL fluorescent estrogen/ER complexes. The negative control was used to determine the polarization value when no competitor was present (theoretical maximum polarization).

The microplate was incubated in the dark at room temperature for 2 h and shaken on a plate shaker. The polarization values were read on a Safire microplate reader and used to calculate the $IC_{50}$ values.

4.2.2. VEGFR-2 kinase inhibitory assay

VEGFR-2 kinase assay was conducted using homogeneous time resolved fluorescence (HTRF) assay (HTRF ® KinEASE™ TK, Cisbio Bioassays, Codolet, France). The general procedures were as following: VEGFR-2 kinase, substrates, ATP and test compound were mixed and incubated in a final buffer with the total volume of 10 μL in 384-well microplate. Wells containing the substrate and the kinase without compound were used as total reaction control. The assay plate was incubated at 30$^{o}$C in the dark for 1 h. Detection was performed with HTRF module of Beckman Coulter detection platform. Inhibition %= [1-(Sample Ratio-Negative Ratio) / (Positive Ratio-Negative Ratio)] ×100%.

4.2.3. MTT assay for anti-proliferative activities

Cells were cultured in RPMI1640 medium (containing 10% (v/v) FBS, 100 U/mL Penicillin and 100 mg/mL Streptomycin) in a 5% $CO_2$-humidified atmosphere at 37$^{o}$C. Cells were trypsinized and seeded at a density of 1 x $10^5$/mL into a 96-well plate (100 mL/well) and incubated at 37$^{o}$C, 5% $CO_2$ atmosphere for 24 h. After this time they were treated with 100 mL/well medium containing test compounds which had been pre-prepared to provide the concentration range of 4 x $10^{-5}$ mol/L, 2 x $10^{-5}$ mol/L, 1 x $10^{-5}$ mol/L, 1 x $10^{-6}$ mol/L, 1 x $10^{-6}$ mol/L and 1 x $10^{-7}$ mol/L, and re-incubated for a further 48 h. Control wells were added the equivalent volume of medium containing 1% (v/v) DMSO. 20 μL MTT (5 mg/mL) was added and cells continued to incubate in darkness at 37$^{o}$C for 4 h. The culture medium was then removed carefully and 150 mL DMSO was added. The cells were maintained at room temperature in darkness for 20 min to ensure thorough color diffusion before reading the absorbance. The absorbance values were read at 490 nm for determination of $IC_{50}$ values.

4.2.4. Real-Time Polymerase Chain Reaction (RT-PCR).

RNA samples were reverse transcribed to cDNA and the PCR reactions were performed using TaKaRa SYBR Green Master Mix (Code. no. 638320) carried out in StepOnePlusTM Real-Time PCR instrument (4376600, Life Technologies). The program for amplification was 1 cycle of 95°C for 2 min followed by 40 cycles of 95°C for 10 s, 60°C for 30 s, and 95°C for 10 s. The PCR results were normalized to GAPDH expression and were quantified by the

$^{\Delta\Delta}$CT method.

4.2.5. Chicken chorioallantoic membrane (CAM) assay

Fertilized eggs were incubated for 7 days in a humidified environment at 37$^{o}$C with 5% $CO_2$ in air and saturated humidity. Then, a window of approximately 1 $cm^2$ was opened on the egg shell to expose the CAM. Test compounds and positive control Sunitinib dissolved in DMSO were placed on sterile methyl cellulose filter papers with phosphate buffered saline as the blank control. The papers were then placed on the CAM. The window was sealed with sterile cellophane tape. The eggs were further incubated at 37$^{o}$C under a constant relative humidity of 60% for 72 h. After fixed with acetone and ethanol for 10min, the CAM was cut and papers removed to observe angiogenesis. Images of the control and sample-treated areas were captured.

4.2.6. Cellular apoptosis study

Annexin V/PI staining assay was used to assess the mechanism of cell death. MCF-7 cells were treated with **II-9OH** at concentration of 10 μM for 48 h. Then, cells were collected, washed with PBS, and stained with annexin V fluorescein isothiocyanate (FITC) and PI for 15 min at RT. After that, the samples were analyzed by flow cytometry using FACScalibur (Becton Dickinson). The cell distributions were calculated using Cell Quest software (Becton Dickinson).

4.2.7. Transwell invasion assay

Invasion assays were performed following the manufacturer's instructions (BD Biosciences). Cells were treated at time of plating. After 24 h (as noted in the legend), invasion cells were fixed to the Matrigel (BD Biosciences)-coated transwell membranes with a seeding density of $5\times10^4$ cells per well for 48 h and stained with crystal violet (0.1 % in 20 % methanol), and invaded cells visualized and quantified by microscopy.

4.2.8. Western Blots.

Cells with different treatments for 24 h were washed twice with PBS, then collected and lysed in lysis buffer (100 mM of Tris-Cl, pH 6.8, 4% (m/v) SDS, 20% (v/v) glycerol, 200 mM of β-mercaptoethanol, 1mM of PMSF, 0.1 mM NaF and DTT) for 1 h on the ice. The lysates were then subjected to centrifugation (13,000 rpm) at 4 °C for 20 min. Protein concentration in the supernatants was detected by BCA protein assay (Thermo, Waltham, MA). Then equal

amount of protein was separated with 12% SDS-PAGE and transferred to polyvinylidene difluoride (PVDF) membranes (Millipore, Bedford, MA) using a semi-dry transfer system (Bio-rad, Hercules, CA). Proteins were detected using specific antibodies overnight at 4°C followed by HRP-conjugated secondary antibodies for 1 h at 37 °C. All of the antibodies were diluted in PBST containing 1% BSA. Enhanced chemiluminescent reagents (Beyotime, Jiangsu, China) were used to detect the HRP on the immunoblots, and the visualized bands were captured by film. The bands were quantified by Quantity One software (Vision 4.62, Bio-rad, Hercules, CA), and the relative protein level were normalized to β-actin.

4.2.9. Molecular modeling

The molecular modeling was performed with Discovery Studio.3.0/CDOCK protocol (Accelrys Software Inc.). The crystal structures of ERα complexed with 4-hydroxytamoxifen (PDB code: 3ERT) and VEGFR-2 (PDB ID code: 3CJF) were downloaded from Protein Data Bank. Compound **II-9OH** was drowned and optimized using Hyperchem v7.0. The protein and ligand were optimized and charged with CHARMm force field to perform docking. Up to 10 conformations were retained, and binding modes presented graphically are representative of the highest-scored conformations.

**Supplementary data**

Supplementary data (the $^{1}$H NMR and $^{13}$C NMR spectra of target compounds associated with this article can be found, in the online version, at.

**Acknowledgements**

This work was supported by grants from the Natural Science Foundation of China (NSFC, 81373279).

**Abbreviations**

ER, estrogen receptor; SERMs, selective estrogen receptor modulators; VEGF, Vascular endothelial growth factor; VEGFR-2, Vascular endothelial growth factor receptor-2; RTK, receptor tyrosine kinase; MAPK, mitogen-activated protein kinase; ERK, extracellular regulated kinases; SAR, structure-activity relationship; HUVEC, human umbilical vein endothelial cell; RT-PCR, real-time polymerase chain reaction; PgR, progesterone receptor; E2, estradiol; MTT, 3-(4,5-dimethylthiazol-2-yl)-2,5-diphenyltetrazolium bromide.

**References and notes**


[1] C. Maurer, S. Martel, D. Zardavas, M. Ignatiadis, New agents for endocrine resistance in breast cancer, The Breast 34 (2017) 1-11.

[2] S. Martinkovich, D. Shah, S.L. Planey, J. Arnott, Selective estrogen receptor modulators: tissue specificity and clinical utility, Clin. Interv. Aging 9 (2014) 1437-1452.

[3] D.P. McDonnell, S.E. Wardell, The molecular mechanisms underlying the pharmacological actions of ER modulators: implications for new drug discovery in breast cancer, Curr. Opin. Pharmacol. 10 (2010) 620-628.

[4] V.C. Jordan, Chemoprevention of breast cancer with selective oestrogen-receptor modulators, Nat. Rev. Cancer 7 (2007) 46-53.

[5] Shagufta, I. Ahmad, Tamoxifen a pioneering drug: An update on the therapeutic potential of tamoxifen derivatives, Eur. J. Med. Chem. 143 (2018) 515-531.

[6] T.L. Wang, Q.D. You, F.S.G. Huang, H. Xiang, Recent Advances in Selective Estrogen Receptor Modulators for Breast Cancer, Mini-Rev. Med. Chem. 9 (2009) 1191-1201.

[7] J.A. Katzenellenbogen, The 2010 Philip S. Portoghese Medicinal Chemistry Lectureship: addressing the "core issue" in the design of estrogen receptor ligands, J. Med. Chem. 54 (2011) 5271-5282.

[8] T. Traboulsi, M. El Ezzy, J.L. Gleason, S. Mader, Antiestrogens: structure-activity relationships and use in breast cancer treatment, J. Mol. Endocrinol. 58 (2017) 15-31.

[9] S.R. Stauffer, C.J. Coletta, R. Tedesco, G. Nishiguchi, K. Carlson, J. Sun, B.S. Katzenellenbogen, J.A. Katzenellenbogen, Pyrazole ligands: structure-affinity/activity relationships and estrogen receptor-alpha-selective agonists, J. Med. Chem. 43 (2000) 4934-4947.

[10] H.B. Zhou, J.S. Comninos, F. Stossi, B.S. Katzenellenbogen, J.A. Katzenellenbogen, Synthesis and evaluation of estrogen receptor ligands with bridged oxabicyclic cores containing a diarylethylene motif: Estrogen antagonists of unusual structure, J. Med. Chem. 48 (2005) 7261-7274.

[11] K. Ohta, T. Ogawa, A. Kaise, Y. Endo, Novel estrogen receptor (ER) modulators containing various hydrophobic bent-core structures, Bioorgan. Med. Chem. 22 (2014) 3508-3514.

[12] R. García-Becerra, N, Santos, L. Díaz, J. Camacho, Mechanisms of Resistance to Endocrine Therapy in Breast Cancer: Focus on Signaling Pathways, miRNAs and Genetically Based Resistance, Int. J. Mol. Sci. 14 (2013) 108-145.

[13] H.A. Abdel-Hafiz, Epigenetic Mechanisms of Tamoxifen Resistance in Luminal Breast Cancer, Diseases, 5 (2017) doi:10.3390/diseases5030016.

[14] S. Ali, M. Rasool, H. Chaoudhry, P. N Pushparaj, P. Jha, A. Hafiz, M. Mahfooz, G. Abdus Sami, M. Azhar Kamal, S. Bashir, A. Ali, M. Sarwar Jamal, Molecular mechanisms and mode of tamoxifen resistance in breast cancer, Bioinformation, 12 (2016) 135-139.

[15] M.E. Fratto, M. Imperatori, B. Vincenzi, F. Tomao, D. Santini, G. Tonini, New perspectives: role of Sunitinib in Breast Cancer, Clin. Ter. 161 (2010) 475-482.

[16] Z. Madak-Erdogan, M. Lupien, F. Stossi, M. Brown, B.S. Katzenellenbogen, Genomic collaboration of estrogen receptor alpha and extracellular signal-regulated kinase 2 in regulating gene and proliferation programs, Mol. Cell. Biol. 31 (2011) 226-236.

[17] J.D. Yan, Y.R. Liu, Z.Y. Zhang, G.Y. Liu, J.H. Xu, L.Y. Liu, Y.M. Hu, Expression and prognostic significance of VEGFR-2 in breast cancer in tumor growth and angiogenesis, Pathol. Res. Pract. 211 (2015) 539-543.

[18] R.R. Patel, S. Sengupta, H.R. Kim, A.J. Klein-Szanto, J.R. Pyle, F. Zhu, T.Y. Li, E.A. Ross, S. Oseni, J. Fargnoli, V.C. Jordan, Experimental treatment of oestrogen receptor (ER) positive breast cancer with tamoxifen and brivanib alaninate, a VEGFR-2/FGFR-1 kinase inhibitor: A potential clinical application of angiogenesis inhibitors, Eur. J. Cancer. 46 (2010) 1537-1553.

[19] J. Kim, H. Kim, and S.B. Park, Privileged Structures: Efficient Chemical "Navigators" toward Unexplored Biologically Relevant Chemical Spaces, J. Am. Chem. Soc. 136 (2014) 14629-14638.

[20] M. Murahari, K.V. Prakash, G.J. Peters, Y.C. Mayur, Acridone-pyrimidine hybrids-design, synthesis, cytotoxicity studies in resistant and sensitive cancer cells and molecular docking studies, Eur. J. Med. Chem. 139 (2017) 961-981.

[21] J. Akhtar, A.A. Khan, Z. Ali, R. Haider, M. Shahar Yar, Structure-activity relationship (SAR) study and design strategies of nitrogen-containing heterocyclic moieties for their anticancer activities, Eur. J. Med. Chem. 139 (2017) 961-981. 125 (2017) 143-189.

[22] P.A. Harris, A. Boloor, M. Cheung, R. Kumar, R.M. Crosby, R.G. Davis-Ward, A.H. Epperly, K.W. Hinkle, R.N. Hunter, J.H. Johnson, V.B. Knick, C.P. Laudeman, D.K. Luttrell, R.A. Mook, R.T. Nolte, S.K. Rudolph, J.R. Szewczyk, A.T. Truesdale, J.M. Veal, L. Wang, J.A. Stafford, Discovery of 5-[[4-[(2, 3-dimethyl-2H-indazol-6-yl)methylamino]-2-pyrimidinyl]amino]-2-methyl-benzenesulfon amide (Pazopanib), a novel and potent vascular endothelial growth factor receptor inhibitor, J. Med. Chem. 51 (2008) 4632-4640.

[23] T.V. Hughes, S.L. Emanuel, A.K. Beck, S.K. Wetter, P.J. Connolly, P. Karnachi, M. Reuman, J. Seraj, A.R. Fuentes-Pesquera, R.H. Gruninger, S.A. Middleton, R. Lin, J.M. Davis, D.F. Moffat, 4-Aryl-5-cyano-2-aminopyrimidines as VEGF-R2 inhibitors: synthesis and biological evaluation, Bioorg. Med. Chem. Lett. 17 (2007) 3266-3270.

[24] M.A. Duncton, E.L. Piatnitski Chekler, R. Katoch-Rouse, D. Sherman, W.C. Wong, L.M. Smith, J.K. Kawakami, A.S. Kiselyov, D.L. Milligan, C. Balagtas, Y.R. Hadari, Y. Wang, S.N. Patel, R.L. Rolster, J.R. Tonr, D. Surguladze, S. Mitelman, P. Kussie, P. Bohlen, J.F. Doody, Arylphthalazines as potent, and orally bioavailable inhibitors of VEGFR-2, Bioorg. Med. Chem. 17 (2009) 731-740.

[25] Z.C. Tang, C.Z. Wu, T.L. Wang, K.J. Lao, Y.J. Wang, L.Y. Liu, M. Muyaba, P. Xu, C.H. He, G.S. Luo, Z.Y. Qian, S.X. Niu, L.J. Wang, Y. Wang, H. Xiao, Q.D. You, H. Xiang, Design, synthesis and evaluation of 6-aryl-indenoisoquinolone derivatives dual targeting ERα and VEGFR-2 as anti-breast cancer agents, Eur. J. Med. Chem. 118 (2016) 328-339.

[26] G.S. Luo, X.Y. Li, G.Q. Zhang, C.Z. Wu, Z.P. Tang, L.Y. Liu, Q.D. You, H. Xiang, Novel SERMs based on 3-aryl-4-aryloxy-2H-chromen-2-one skeleton - A possible way to dual ERα/VEGFR-2 ligands for treatment of breast cancer, Eur. J. Med. Chem. 140 (2017) 252-273.

[27] A.M. Brzozowski, A.C. Pike, Z. Dauter, R.E. Hubbard, T. Bonn, O. Engström, L. Ohman, G.L. Greene, J.A. Gustafsson, M. Carlquist, Molecular basis of agonism and antagonism in the oestrogen receptor, Nature 389 (1997) 753-758.

[28] C.A. Sehon, G.Z. Wang, A.Q. Viet, K.B. Goodman, S.E. Dowdell, P.A. Elkins, S.F. Semus, C. Evans, L.J. Jolivette, R.B. Kirkpatrick, E. Dul, S.S. Khandekar, T. Yi, L.L. Wright, G.K. Smith, D.J. Behm, R. Bentley, C.P. Doe, E. Hu, D. Lee, Potent, Selective and Orally Bioavailable Dihydropyrimidine Inhibitors of Rho Kinase (ROCK1) as Potential Therapeutic Agents for Cardiovascular Diseases, J. Med. Chem. 51 (2008) 6631-6634.

[29] G.M. Anstead, K.E. Carlson, J.A. Katzenellenbogen, The estradiol pharmacophore: ligand structure-estrogen receptor binding affinity relationships and a model for the receptor binding site, Steroids 62 (1997) 268-303.

[30] M. Simons, E. Gordon, L. Claesson-Welsh, Mechanisms and regulation of endothelial VEGF receptor signaling, Nat. Rev. Mol. Cell. Biol. 17 (2016) 611-625.

[31] W. Chen, G.X. Zhang, L. Guo, W.X. Fan, Q. Ma, X.D. Zhang, R.L. Du, R.H. Cao, Synthesis and biological evaluation of novel alkyl diamine linked bivalent b-carbolines as angiogenesis inhibitors, Eur. J. Med. Chem. 124 (2016) 249-261

[32] A. Maiti, K. Takabe, N.C. Hait, Metastatic triple-negative breast cancer is dependent on SphKs/S1P signaling for growth and survival, Cell Signal. 32 (2017) 85-92.

[33] Y.V. Kuznetsov, I.S. Levina, A.M. Scherbakov, O.E. Andreeva, I.V. Fedyushkina, A.S. Dmitrenok, A.S. Shashkov, I.V. Zavarzin, New estrogen receptor antagonists. 3,20-Dihydroxy-19-norpregna-1,3,5(10)-trienes: Synthesis, molecular modeling, and biological evaluation, Eur. J. Med. Chem. 143 (2018) 670-682

# Highlights

- Twenty-one pyrimidines were evaluated as dual ERα/VEGFR-2 ligands
- **II-9OH** exhibited potent activities in both enzymatic and cellular assays
- **II-9OH** induced apoptosis and inhibited migration on MCF-7 cells
- *In vivo* anti-angiogenic activity of **II-9OH** was determined using CAM assay.
- Synergetic effect of **II-9OH** on ERα and VEGFR-2/Raf-1/MAPK/ERK pathway.